



*Peter Schuck
(1940-2022)*

Equation of motion approach to nuclear structure

Elena Litvinova



Western Michigan University



MICHIGAN STATE
UNIVERSITY



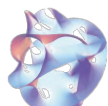
Collaborators: *Peter Schuck, Peter Ring, Manqoba Hlatshwayo,
Yinu Zhang, Caroline Robin, Herlik Wibowo*

*INT 23-1a Program "Intersection of nuclear structure and high-energy nuclear collisions",
Seattle, January 23 - February 24, 2023*

Hierarchy of energy scales and nuclear many-body problem

Degrees of freedom Energy [MeV]

String theory



strings

>10⁶



quarks, gluons

QCD



constituent quarks

940
neutron mass

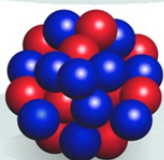
$m_\omega \approx 783$ MeV
 $m_\rho \approx 770$ MeV
 $m_\sigma \approx 500$ MeV
 $m_\pi \approx 140$ MeV

“ab initio”



baryons, mesons

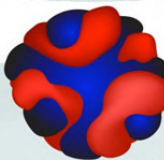
Configuration Interaction (CI)



protons, neutrons

8
proton separation
energy in lead

Density Functional Theory (DFT)



nucleonic densities
and currents

1.12
vibrational
state in tin

Collective coordinates (CC)



collective coordinates

0.043
rotational
state in uranium

Atomic theory



electrons

13.6×10^{-6}
binding energy of H-atom

• **The major conflict:**

Separation of energy scales => effective field theories

VS

The physics on a certain scale is governed by the next higher-energy scale

Hamiltonian:

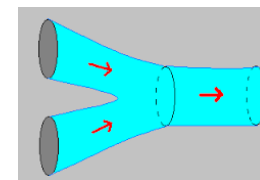
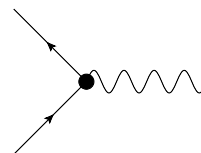
$$H = K + V$$

center of mass

internal degrees of freedom:
next energy scale

Standard Model:
free propagation and
interaction (input)

String theory:
merging strings
NO “Interaction”

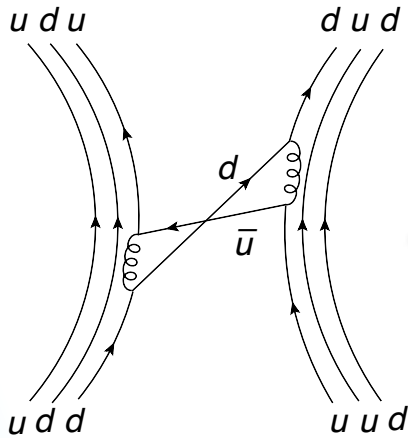


• **Possible solution:**

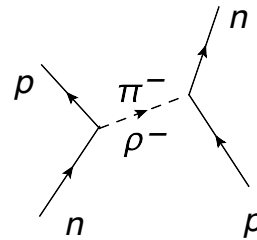
- Keep/establish connections between the scales via **emergent phenomena**
- A universal approach to the strongly-coupled QMBP?

The underlying mechanism of NN-interaction:

Quantum Chromodynamics (QCD, high energy)

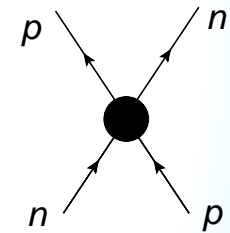


Quantum Hadrodynamics (QHD, intermediate energy)



Relay of EFTs:

Nuclear Structure (NS, low energy)



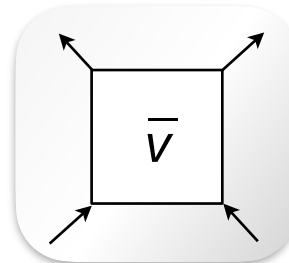
QCD

QHD

NS

Formalism:

- Generic bare "interaction": model-independent, all channels included
- Higher-orders are treated via **in-medium propagators**
- No perturbation theory



In implementations:

- Meson-exchange (ME) at leading order
- Effective coupling constants/masses (adjusted on the mean-field (MF) level) + subtraction of beyond-MF double-counting
- Bare ME + subtraction of MF artifacts (in progress)

A strongly-correlated many body system: single-fermion propagator, particle-hole propagator and related observables

$$H = \sum_{12} \bar{\psi}_1 (-i\gamma \cdot \nabla + M)_{12} \psi_2 + \frac{1}{4} \sum_{1234} \bar{\psi}_1 \bar{\psi}_2 \bar{v}_{1234} \psi_4 \psi_3 = T + V^{(2)}$$

Hamiltonian,
extendable to 3-body
etc.

$$G_{11'}(t - t') = -i \langle T \psi(1) \bar{\psi}(1') \rangle \quad 1 = \{\xi_1, t\}$$

**Single-particle
propagator**

Fourier transform:
Spectral
expansion

$$G_{11'}(\varepsilon) = \sum_n \frac{\eta_1^n \bar{\eta}_{1'}^{n*}}{\varepsilon - \varepsilon_n^+ + i\delta} + \sum_m \frac{\chi_1^m \bar{\chi}_{1'}^{m*}}{\varepsilon + \varepsilon_m^- - i\delta}$$

Residues - spectroscopic
(occupation) factors

$$\eta_1^n = \langle 0^{(N)} | \psi_1 | n^{(N+1)} \rangle \quad \chi_1^m = \langle m^{(N-1)} | \psi_1 | 0^{(N)} \rangle$$

Ground state of
N particles

(Excited) state
of (N+1) particles

Poles - single-particle
energies

$$R_{12,1'2'}(t - t') = -i \langle T (\bar{\psi}_1 \psi_2)(t) (\bar{\psi}_{2'} \psi_{1'})(t') \rangle$$

**Particle-hole response
function**

Fourier transform: Spectral
expansion

$$R_{12,1'2'}(\omega) = \sum_{\nu > 0} \left[\frac{\rho_{21}^\nu \bar{\rho}_{2'1'}^{\nu*}}{\omega - \omega_\nu + i\delta} - \frac{\bar{\rho}_{12}^{\nu*} \rho_{1'2'}^\nu}{\omega + \omega_\nu - i\delta} \right]$$

Residues - transition
densities

Excitation
energies

$$\rho_{12}^\nu = \langle 0 | \bar{\psi}_2 \psi_1 | \nu \rangle$$

Poles - excitation energies



Exact equations of motion (EOM) for binary interactions: one-body problem

One-fermion propagator

$$G_{11'}(t - t') = -i \langle T \psi(1) \bar{\psi}(1') \rangle$$

EOM: Dyson Eq.

$$G(\omega) = G^{(0)}(\omega) + G^{(0)}(\omega) \Sigma(\omega) G(\omega) \quad (*) \quad \Sigma(\omega) = \Sigma^{(0)} + \Sigma^{(r)}(\omega)$$

Irreducible kernel (Self-energy, exact):

Instantaneous term (Hartree-Fock incl. "tadpole")
Short-range correlations

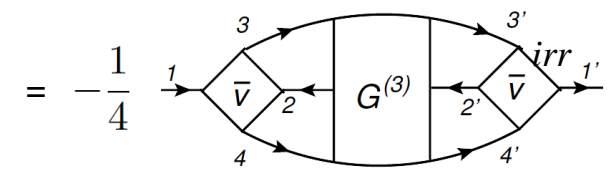
$$\Sigma_{11'}^{(0)} = -\langle \gamma^0 \{ [V, \psi_1], \bar{\psi}_{1'} \} \gamma^0 \rangle$$

$$= \sum_{22'} \bar{v}_{121'2'} \langle \bar{\psi}_2 \psi_{2'} \rangle = \text{Diagram: } \begin{array}{c} \text{circle with } \rho_{2'2} \text{ and arrow} \\ \text{square with } \bar{v} \end{array}$$

t-dependent (dynamical) term (symmetric version): **Long-range correlations**

$$\Sigma_{11'}^{(r)} = i \langle T \gamma^0 [V, \psi_1](t) [V, \bar{\psi}_{1'}](t') \gamma^0 \rangle^{irr}$$

$$= -\frac{1}{4} \sum_{234} \sum_{2'3'4'} \bar{v}_{1234} G_{432', 23'4'}^{(3)irr}(t - t') \bar{v}_{4'3'2'1'}$$



$$\rho_{11'} = -i \lim_{t=t'-0} G_{11'}(t - t')$$

is the full solution of (*):
includes the dynamical term!

Koltun-Migdal-Galitsky sum rule: **the binding energy**

"Ab-initio DFT":

$$E_0 = \frac{1}{2\pi} \int_{-\infty}^{\bar{\epsilon}_F} d\epsilon \sum_{12} (T_{12} + \epsilon \delta_{12}) \text{Im} G_{21}(\epsilon)$$

Equation of motion (EOM) for the particle-hole response

Particle-hole propagator
(response function):

$$R_{12,1'2'}(t-t') = -i \langle T(\bar{\psi}_1 \psi_2)(t) (\bar{\psi}_{2'} \psi_{1'})(t') \rangle$$

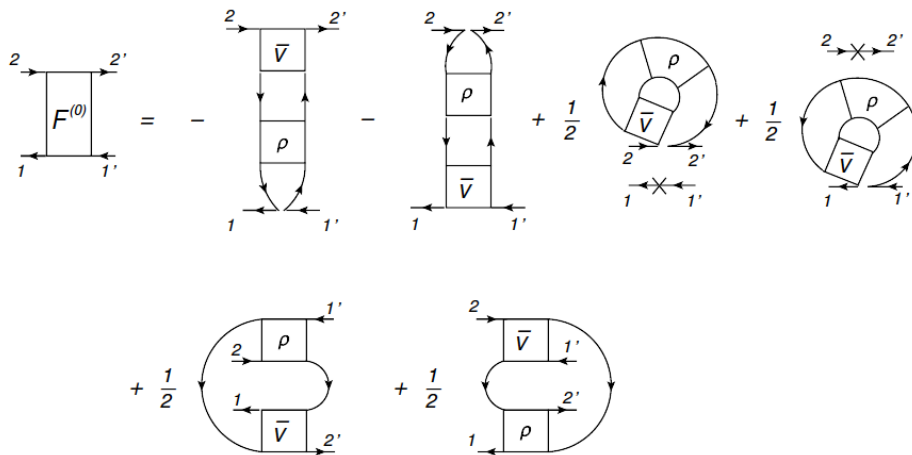
spectra of excitations,
masses, decays, ...

EOM: Bethe-Salpeter-Dyson Eq.

$$R(\omega) = R^{(0)}(\omega) + R^{(0)}(\omega)F(\omega)R(\omega) \quad (**) \quad F(t-t') = F^{(0)}\delta(t-t') + F^{(r)}(t-t')$$

Irreducible kernel (exact):

Instantaneous term (“bosonic” mean field):
Short-range correlations

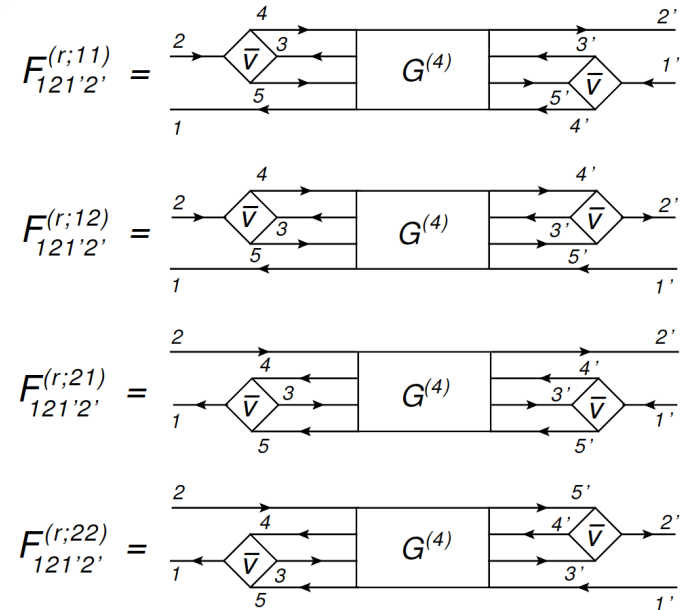


Self-consistent mean field $F^{(0)}$, where

$$\rho_{12,1'2'} = \delta_{22'}\rho_{11'} - i \lim_{t' \rightarrow t+0} R_{2'1,21'}(t-t')$$

contains the full solution of (**) including the dynamical term!

t -dependent (dynamical) term:
Long-range correlations



$$F_{12,1'2'}^{(r)}(t-t') = \sum_{ij} F_{12,1'2'}^{(r;ij)}(t-t')$$

Non-perturbative treatment of two-point $G^{(n)}$ in the dynamical kernels

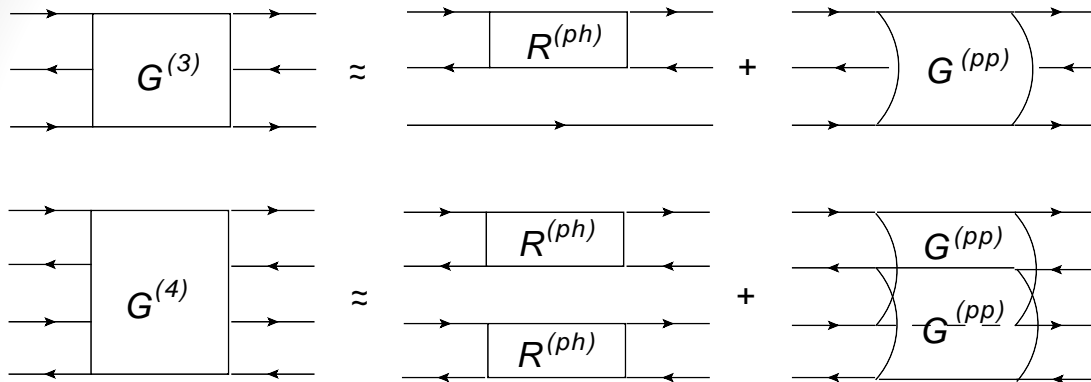
• **Quantum many-body problem in a nutshell:** Direct EOM for $G^{(n)}$ generates $G^{(n+2)}$ in the (symmetric) dynamical kernels and further high-rank correlation functions (CFs); an equivalent of the BBGKY hierarchy. $N_{\text{Equations}} = N_{\text{Particles}} \& \text{ Coupled}$ 🙈 !!! *Truncation on two-body level*

“Self-consistent GFs” This work

• **Non-perturbative solution:**
Cluster decomposition

$$\blacklozenge G^{(3)} = G^{(1)} G^{(1)} G^{(1)} + G^{(2)} G^{(1)} + \Xi^{(3)}$$

$$\blacklozenge G^{(4)} = G^{(1)} G^{(1)} G^{(1)} G^{(1)} + G^{(2)} G^{(2)} + \cancel{G^{(3)} G^{(1)}} + \cancel{\Xi^{(4)}}$$



• P. C. Martin and J. S. Schwinger, *Phys. Rev.* 115, 1342 (1959).

• N. Vinh Mau, *Trieste Lectures* 1069, 931 (1970)

• P. Danielewicz and P. Schuck, *Nucl. Phys.* A567, 78 (1994)

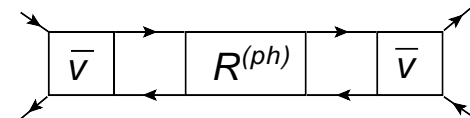
• ...

Exact mapping: particle-hole ($2q$) quasibound states

Emergence of effective “particles” (phonons, vibrations):



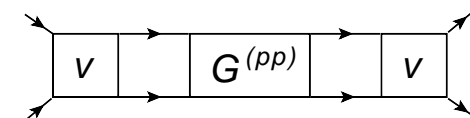
=



Emergence of superfluidity:

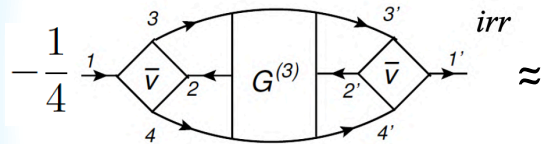


=

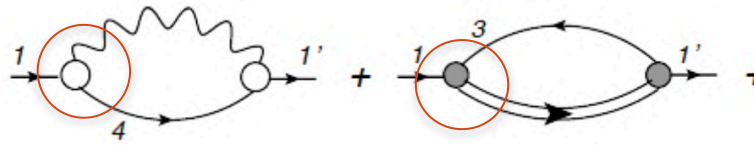


Emergence of effective degrees of freedom

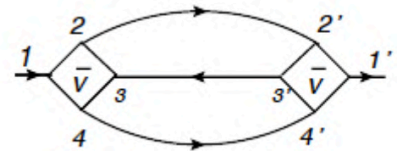
Dynamical self-energy $\Sigma^{(r)}$:



“Radiative-correction”



Second-order



Quasiparticle-vibration coupling (QVC)

Emergent phonon vertices and propagators: *calculable from the underlying H*, which does not contain phonon degrees of freedom

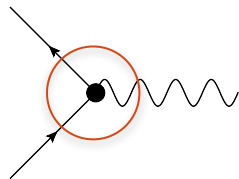
$$H = \sum_{12} h_{12} \psi_1^\dagger \psi_2 + \frac{1}{4} \sum_{1234} \bar{v}_{1234} \psi_1^\dagger \psi_2^\dagger \psi_4 \psi_3$$

“Ab-initio”

$$H = \sum_{12} \tilde{h}_{12} \psi_1^\dagger \psi_2 + \sum_{\lambda\lambda'} \mathcal{W}_{\lambda\lambda'} Q_\lambda^\dagger Q_{\lambda'} + \sum_{12\lambda} [\Theta_{12}^\lambda \psi_1^\dagger Q_\lambda^\dagger \psi_2 + h.c.]$$

Effective QVC

Cf.: The Standard Model elementary interaction vertices: boson-exchange interaction is the *input*:



$$\gamma, g, W^\pm, Z^0$$

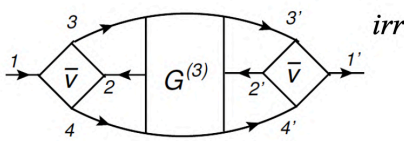
Possibly derivable?

E.L., P. Schuck, PRC 100, 064320 (2019)

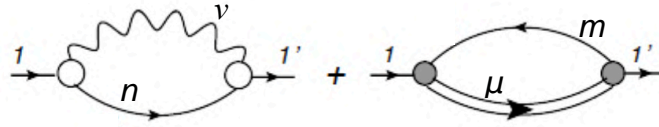
E.L., Y. Zhang, PRC 104, 044303 (2021)

Problems with approximate treatments: poles “mismatch”, (non)-positivity and optical theorem

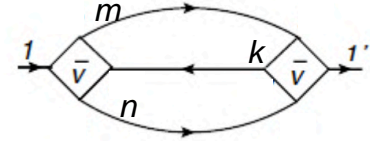
Dynamical self-energy:



“Radiative-correction”



Second-order



Approximate:

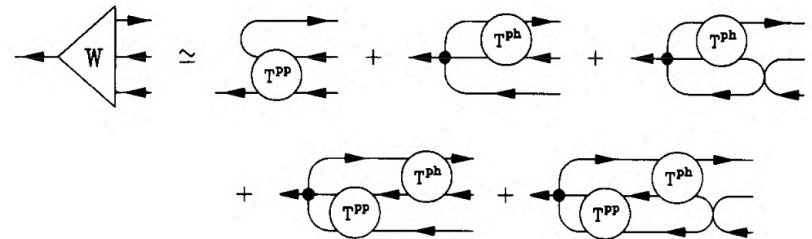
$$\Sigma_{11'}^{(r)+}(\omega) = \sum_{33'} \sum_{\nu n} \frac{\eta_3^n g_{13}^\nu g_{1'3'}^{\nu*} \eta_{3'}^{n*}}{\omega - \omega_\nu - \varepsilon_n^{(+)} + i\delta} + \sum_{22'} \sum_{\mu m} \frac{\chi_2^{m*} \gamma_{12}^{\mu(+)} \gamma_{1'2'}^{\mu(+)*} \chi_{2'}^m}{\omega - \omega_\mu^{(++)} - \varepsilon_m^{(-)} + i\delta} - \sum_{mnk} \frac{w_1^{mnk} w_{1'}^{mnk*}}{\omega - \varepsilon_m^+ - \varepsilon_n^+ - \varepsilon_k^- + i\delta}$$

Exact:

$$\Sigma_{11'}^{(r)+}(\omega) \sim \langle v G^{(3)+}(\omega) v \rangle_{11'}$$

• Watson-Faddeev series:
P. Danielewicz and P. Schuck,
Nucl. Phys. A567, 78 (1994):

$$G_{432', 23'4'}^{(3)+}(\omega) = \sum_{\kappa} \frac{\langle 0 | \bar{\psi}_2 \psi_4 \psi_3 | \kappa \rangle \langle \kappa | \bar{\psi}_3' \bar{\psi}_4' \psi_2' | 0 \rangle}{\omega - \omega_\kappa + i\delta}$$

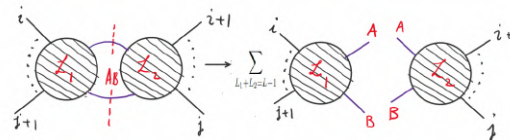


• 2p1h-RPA

P. Schuck, F. Villars and P. Ring
Nucl. Phys. A208, 302 (1973)

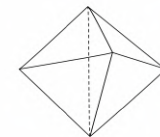
Scattering amplitudes in particle physics
(Yang-Mills theories etc.):

- Positivity preserved when eliminating all the virtual particles
- Amplitudes \Leftrightarrow Polyhedron “living” in the kinematic space
- Emergent unitarity



N. Arkani-Hamed, J. Trnka, A. Hodges et al.

Amplitude is a volume of polyhedron



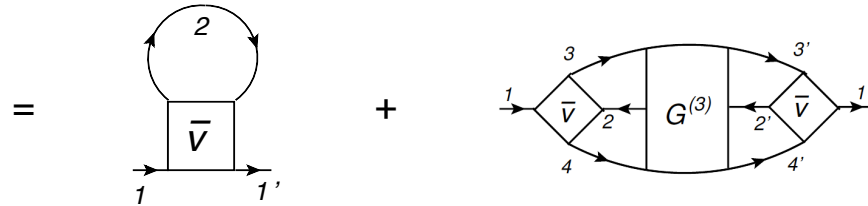
Each face labeled by $\langle abcd \rangle$

$$\frac{\langle 1345 \rangle^3}{\langle 1234 \rangle \langle 1245 \rangle \langle 2345 \rangle \langle 1235 \rangle} \quad \frac{\langle 1356 \rangle^3}{\langle 1235 \rangle \langle 1256 \rangle \langle 2356 \rangle \langle 1236 \rangle}$$

Mean field approximation and beyond

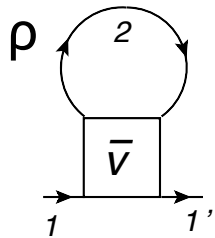
Exact "ab-initio" self-energy :

$$\Sigma_{11'}(\omega) = \Sigma_{11'}^{(0)} + \Sigma_{11'}^{(r)}(\omega)$$



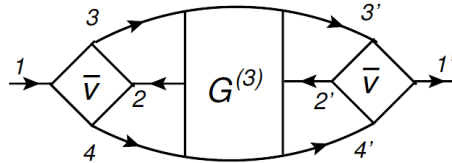
Mean field approximation (density functional theory, DFT)

$$\Sigma_{11'}(\omega) =$$



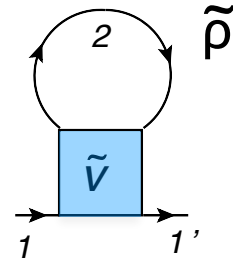
static

+



ω -dependent

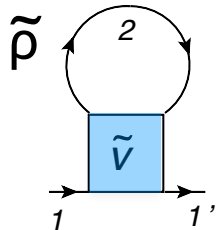
\approx



DFT: static [$\omega = \tilde{\epsilon}_1$ (?)]

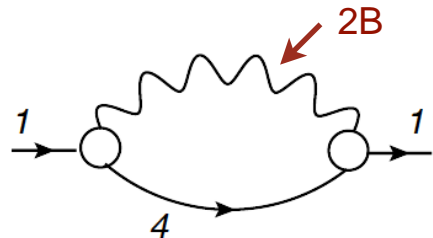
Beyond mean field: particle-vibration coupling (PVC), leading approximation:

$$\Sigma_{11'}(\omega) =$$



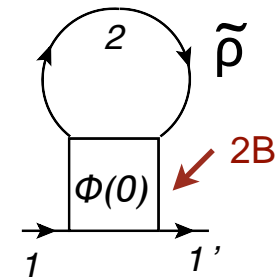
DFT: static, basis

+



PVC ω -dependent

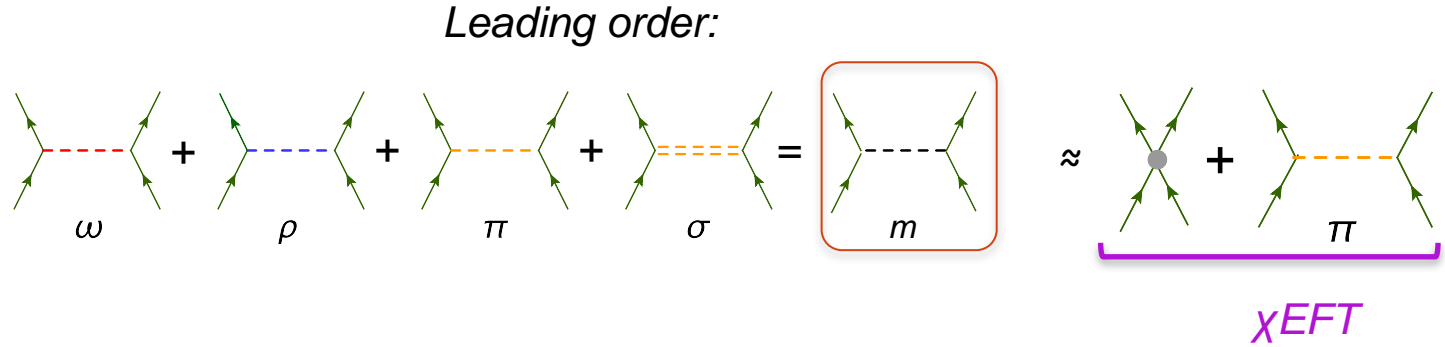
-



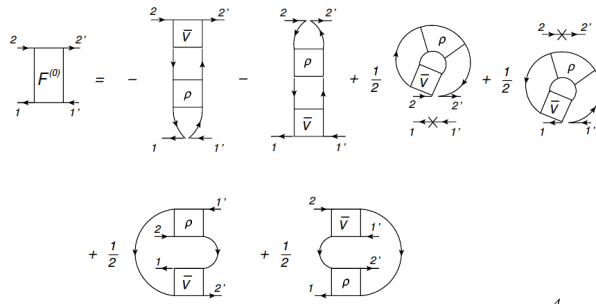
PVC double counting removal

Comparison to the chiral EFT

Quantum Hadrodynamics (QHD)



Relativistic Nuclear Field theory: non-PT, in-medium



Static

+ Dynamical

$$F_{121'2'}^{(r;11)} = \dots$$

$$F_{121'2'}^{(r;12)} = \dots$$

$$F_{121'2'}^{(r;21)} = \dots$$

$$F_{121'2'}^{(r;22)} = \dots$$

+ Dynamical

χ EFT: PT in the vacuum

	Two-nucleon force	Three-nucleon force	Four-nucleon force
LO (Q^0)		—	—
NLO (Q^2)		—	—
N ² LO (Q^4)			—
N ³ LO (Q^6)			
N ⁴ LO (Q^8)			

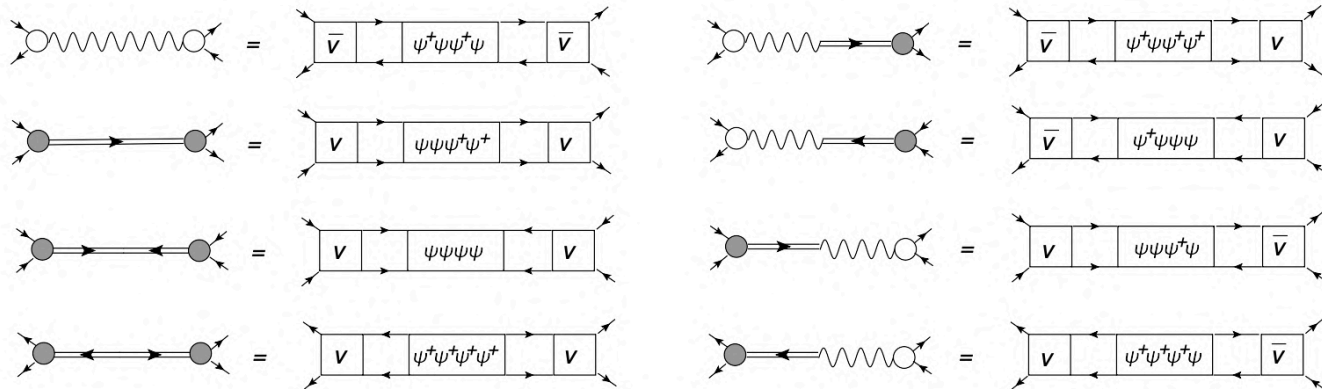
E. Epelbaum et al., Front. Phys. 8, 98 (2020)

“Standard” many-body methods? Is that correct for medium-heavy nuclei?

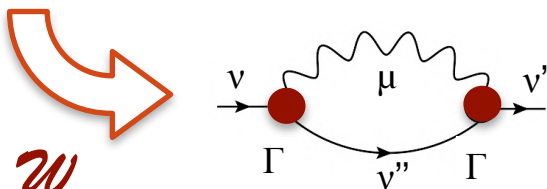
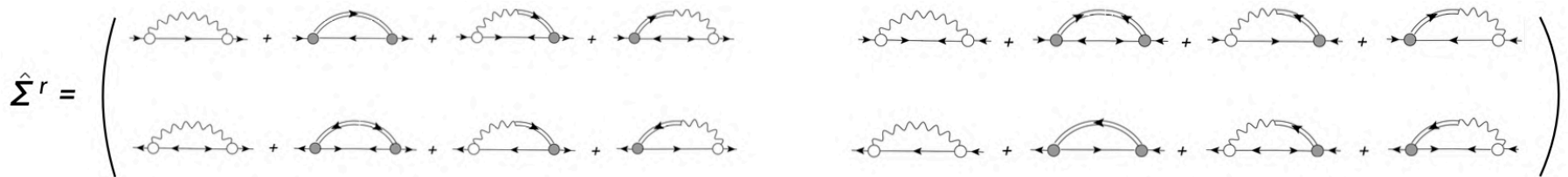
QVC in superfluid systems: dynamical extension of the Gor'kov/HFB theory

Superfluid dynamical kernel: adding particle-number violating contributions

Mapping on the QVC in the canonical basis



Quasiparticle dynamical self-energy (matrix): normal and pairing phonons are unified



Bogoliubov transformation

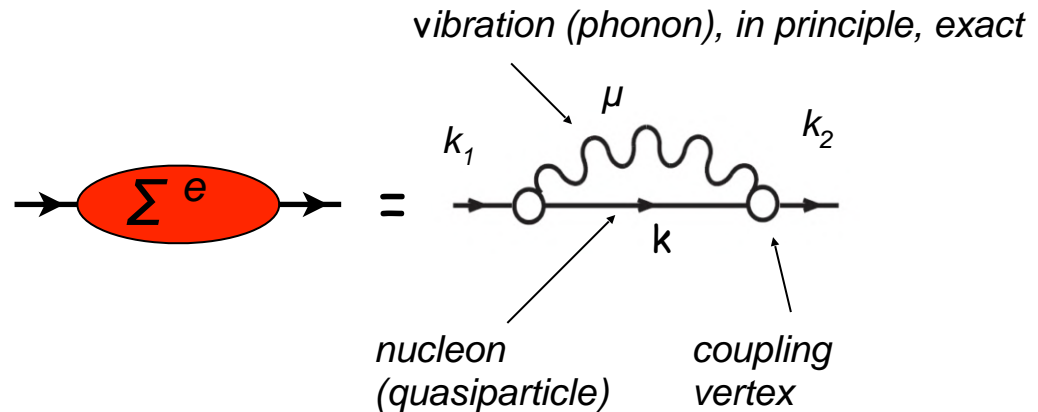
E.L., Y. Zhang, PRC 104, 044303 (2021)
Y. Zhang et al., PRC 105, 044326 (2022)

Cf.: Quasiparticle static self-energy (matrix) in HFB

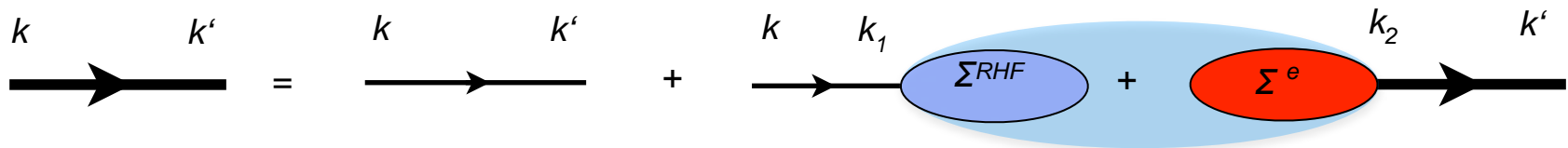
$$\hat{\Sigma}^0 = \begin{pmatrix} \tilde{\Sigma}_{11'} & \Delta_{11'} \\ -\Delta_{11'}^* & -\tilde{\Sigma}_{11'}^T \end{pmatrix}$$

Beyond Hartree-Fock-Bogoliubov: quasiparticle-vibration coupling (QVC)

Dynamical self-energy with energy dependence in the Nambu-Bogoliubov space [e.g., in Hartree-(Fock)-Bogoliubov basis]



One-body propagator G : Dyson equation for Gor'kov Green function



$$G(\varepsilon) = G_0(\varepsilon) + G_0(\varepsilon) [\Sigma^{RHF} + \Sigma^e(\varepsilon)] G(\varepsilon)$$

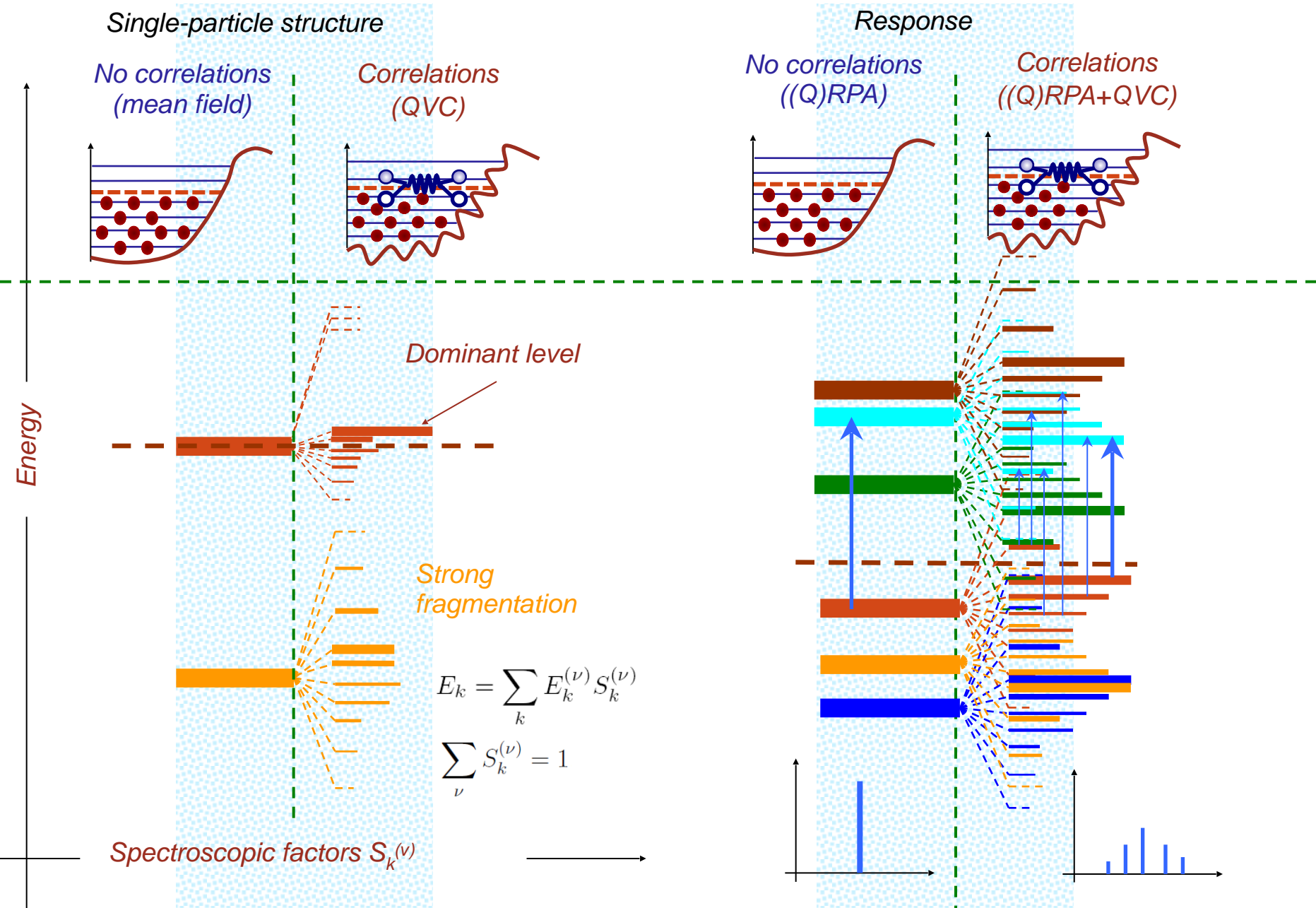
$$\Sigma_{k_1 k_2}^{(e)\eta_1 \eta_2}(\varepsilon) = \sum_{\eta=\pm 1} \sum_{k, \mu} \frac{\gamma_{\mu; k_1 k}^{\eta; \eta_1 \eta} \gamma_{\mu; k_2 k}^{\eta; \eta_2 \eta^*}}{\varepsilon - \eta(E_k + \Omega_\mu - i\delta)}$$

$$\eta = \pm 1$$

forward / backward components in the Nambu-Bogoliubov space

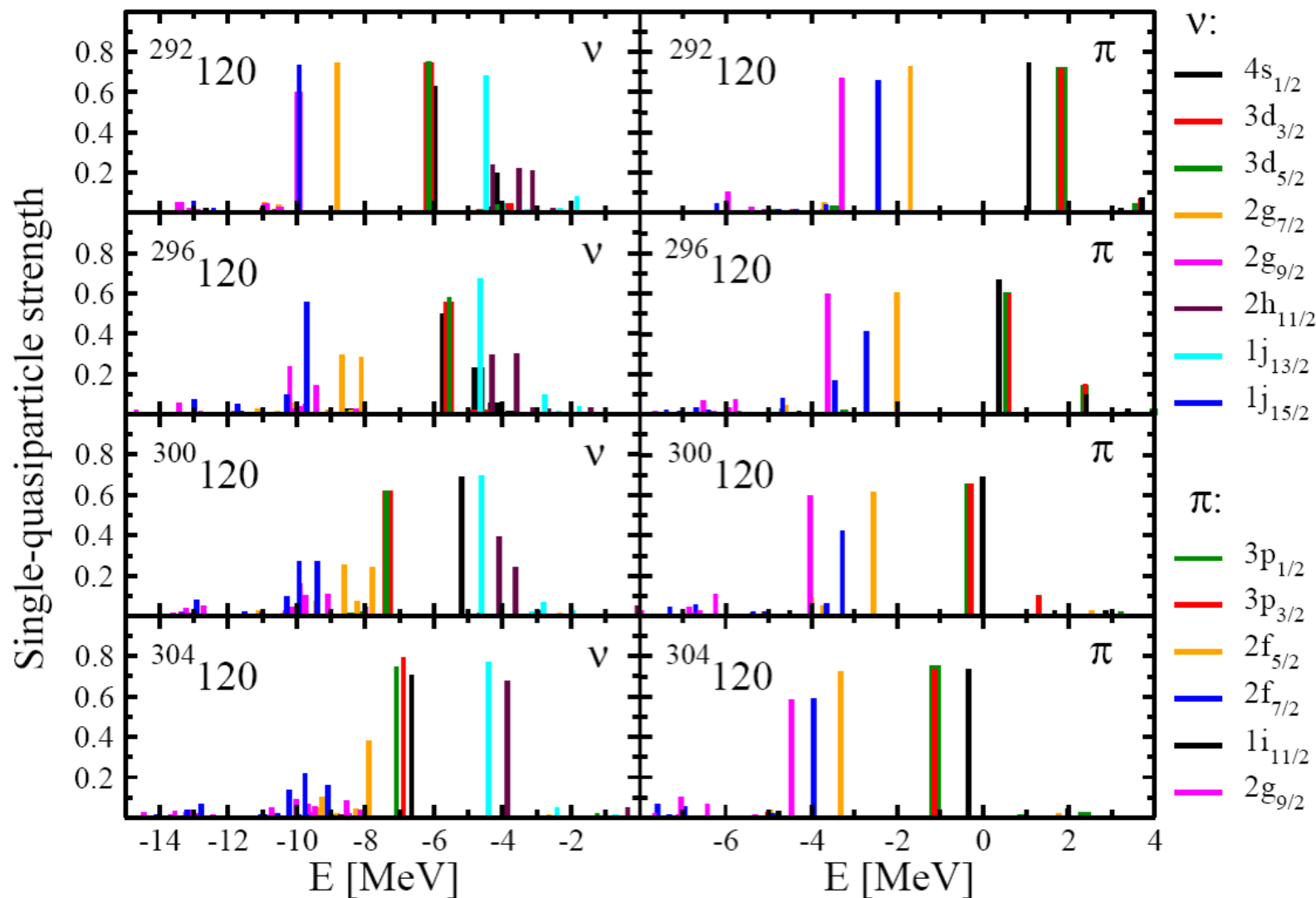
Contrary to QED/QCD, Σ^e converges in nuclei (finite phonon spectrum)

Fragmentation of single-particle states and particle-hole excitations



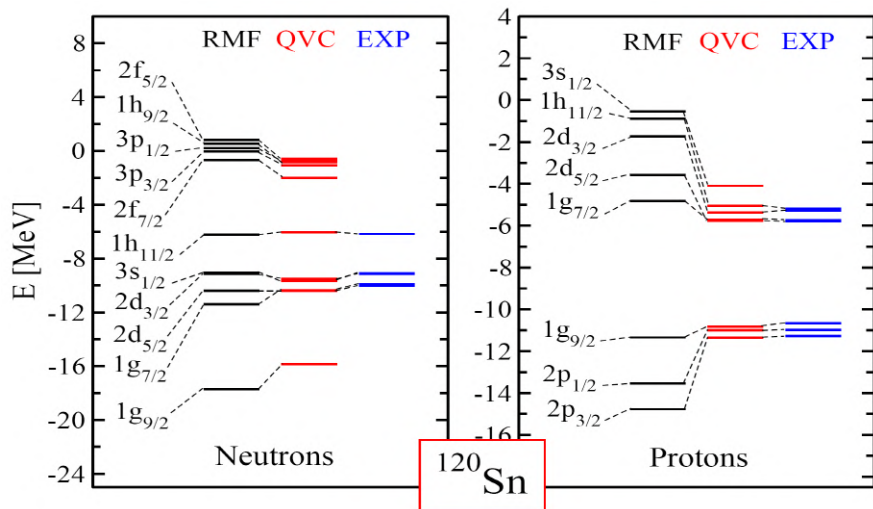
(Quasi)particle-vibration coupling (QVC, PVC):
 Pairing correlations of the superfluid type + coupling to phonons

Full s.p. strength distributions in $Z=120$ nuclei around E_F



(Quasi)particle-vibration coupling (QVC, PVC): Pairing correlations of the superfluid type + coupling to phonons

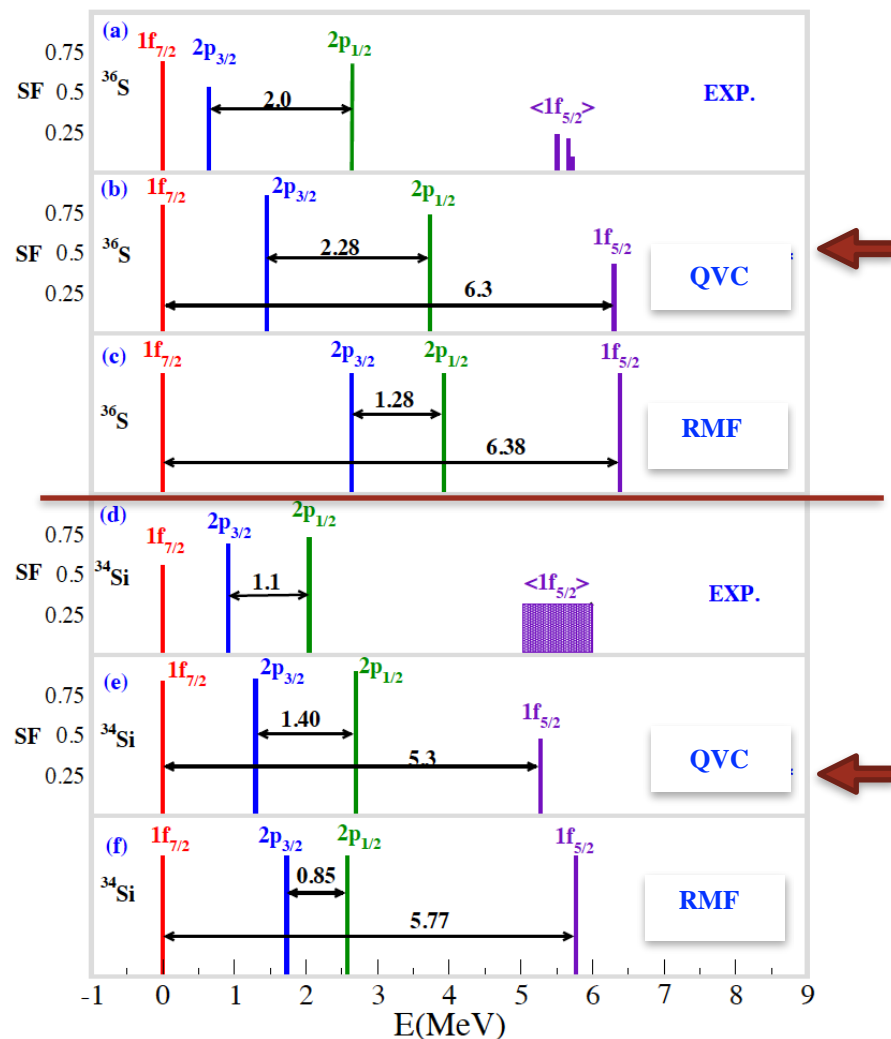
Dominant states and spectroscopic factors in ^{120}Sn :



(nlj) v	S^{th}	S^{exp}
$2d_{5/2}$	0.32	0.43
$1g_{7/2}$	0.40	0.60
$2d_{3/2}$	0.53	0.45
$3s_{1/2}$	0.43	0.32
$1h_{11/2}$	0.58	0.49
$2f_{7/2}$	0.31	0.35
$3p_{3/2}$	0.58	0.54

E. L., P. Ring, PRC 73, 044328 (2006)
E.L., PRC 85, 021303(R) (2012)

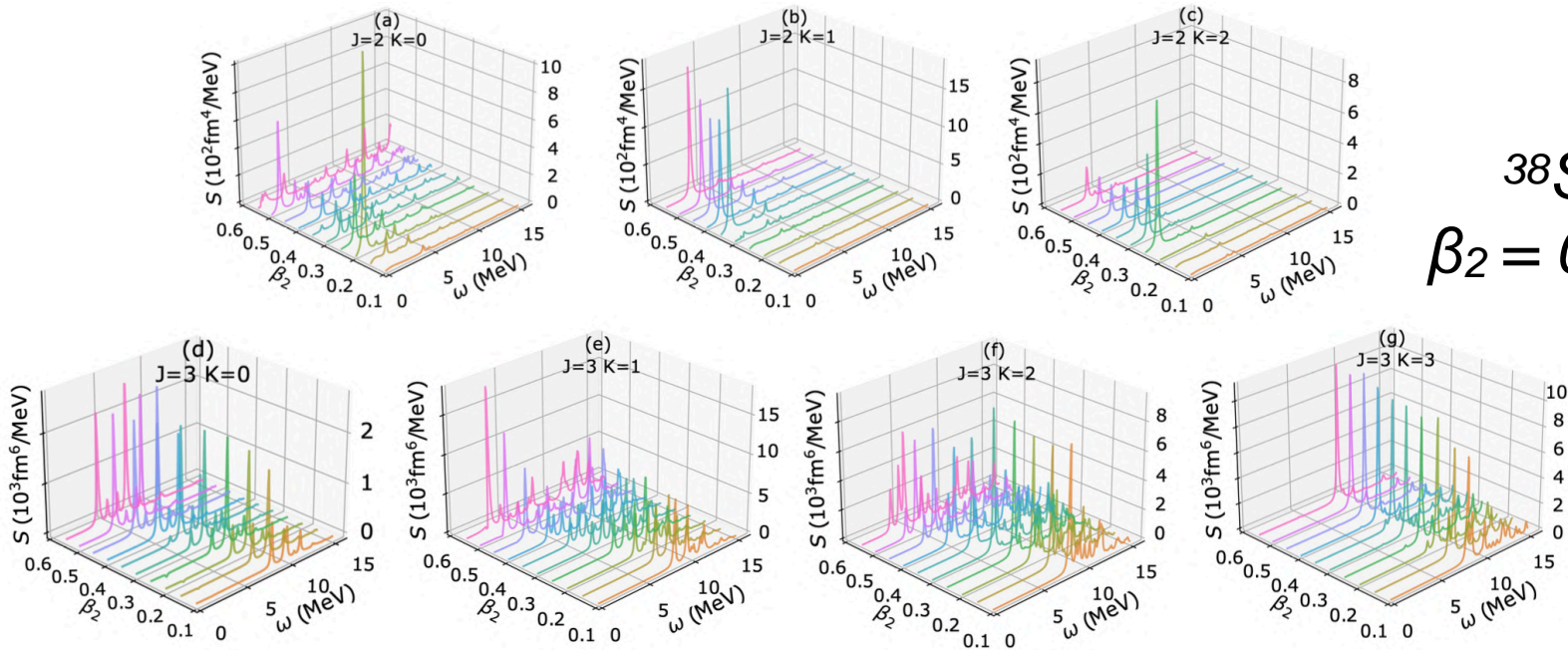
Spin-orbit splittings in ^{36}S
vs a bubble nucleus ^{34}Si ; neutron states:



Exp: Burgunder et al., PRL 112, 042502 (2014)
Th: K. Karakatsanis et al., PRC 95, 034901 (2017)

Single-(quasi)particle states. New implementation: FAM-QRPA+QVC

(i) Relativistic meson-nucleon Lagrangian + (ii) Relativistic Hartree-Bogoliubov (RHB) + (iii) Quasiparticle random phase approximation (QRPA): $J = 2^+ - 5^-$, $K = [0, J]$. Finite amplitude method (FAM): A. Bjelčić et al., CPC 253, 107184 (2020). Relativistic DD-PC1 interaction.



(iv) QVC vertex extraction:

$$\Gamma_{\mu\mu'}^{(ij)n} = \frac{1}{\langle n|F^\dagger|0\rangle} \oint_{\gamma_n} \delta H_{\mu\mu'}^{ij}(\omega) \frac{d\omega}{2\pi i}$$

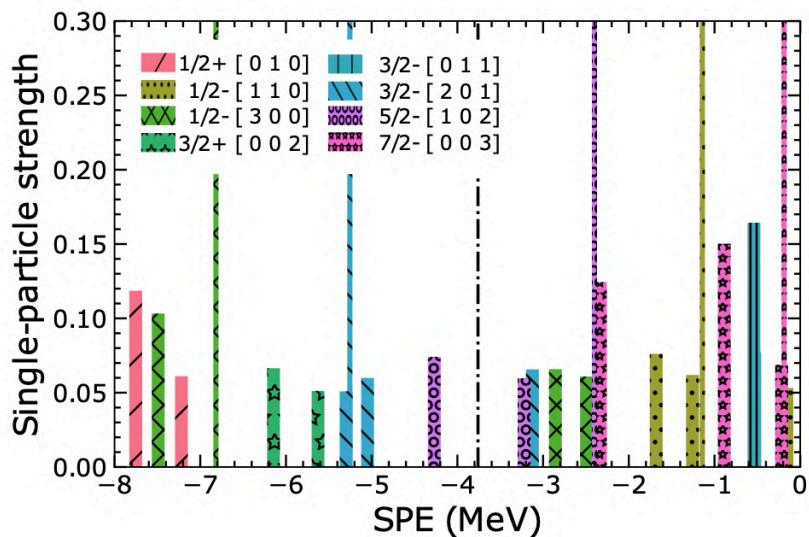
Variation of the HFB Hamiltonian at the QRPA pole

(v) Dyson Eq. solution

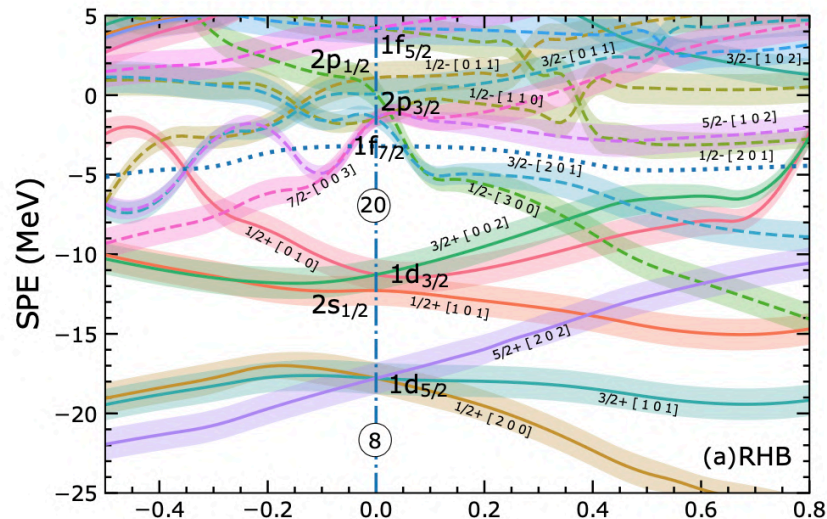
E.L., Y. Zhang, PRC 104, 044303 (2021)

Single-(quasi)particle states in ^{38}Si

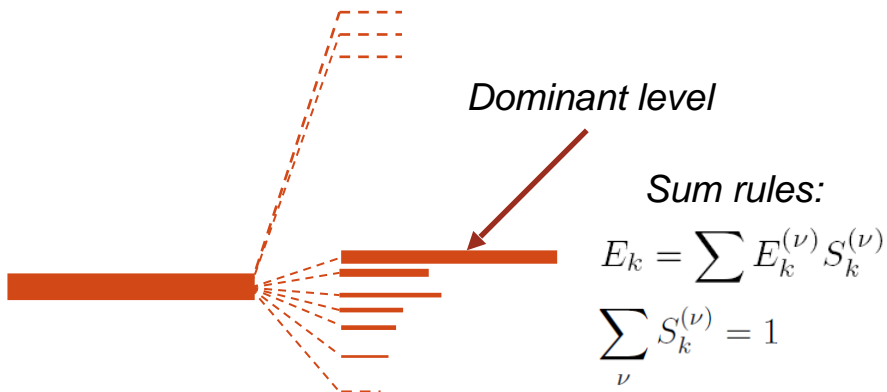
Fragmentation of quasiparticle states:
RHB vs RHB+QVC



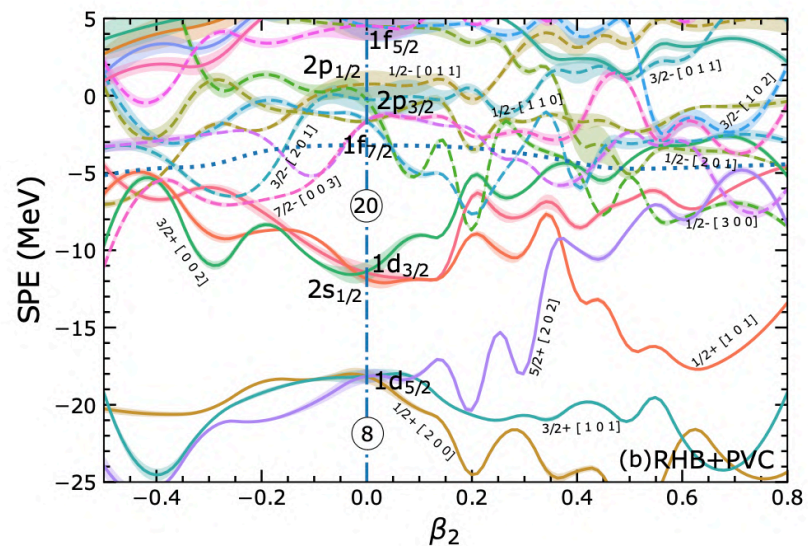
Nilsson diagram: RHB



Fragmentation mechanism: schematic



Nilsson diagram: RHB+QVC (dominant only)



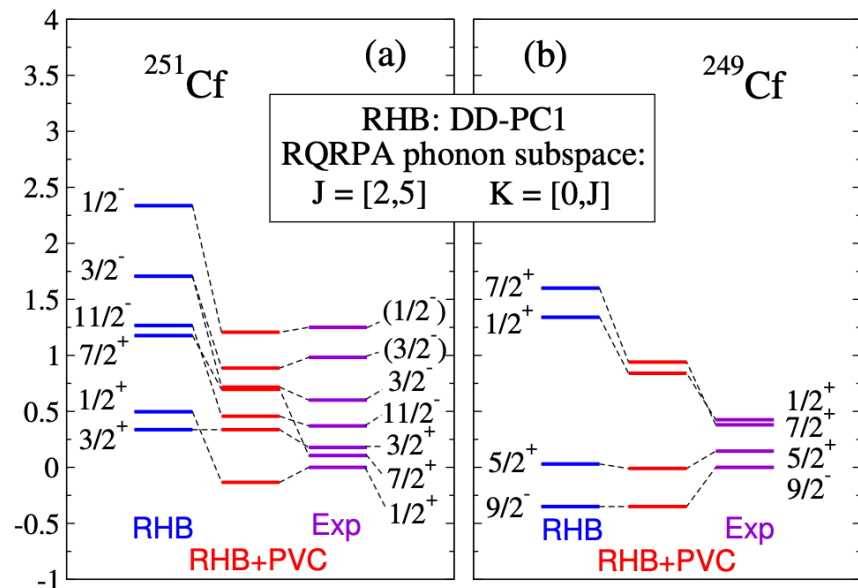
Single-(quasi)particle states in $^{249,251}\text{Cf}$

A. Afanasjev et al.: Long-standing problem of the description of single-particle states in deformed nuclei.

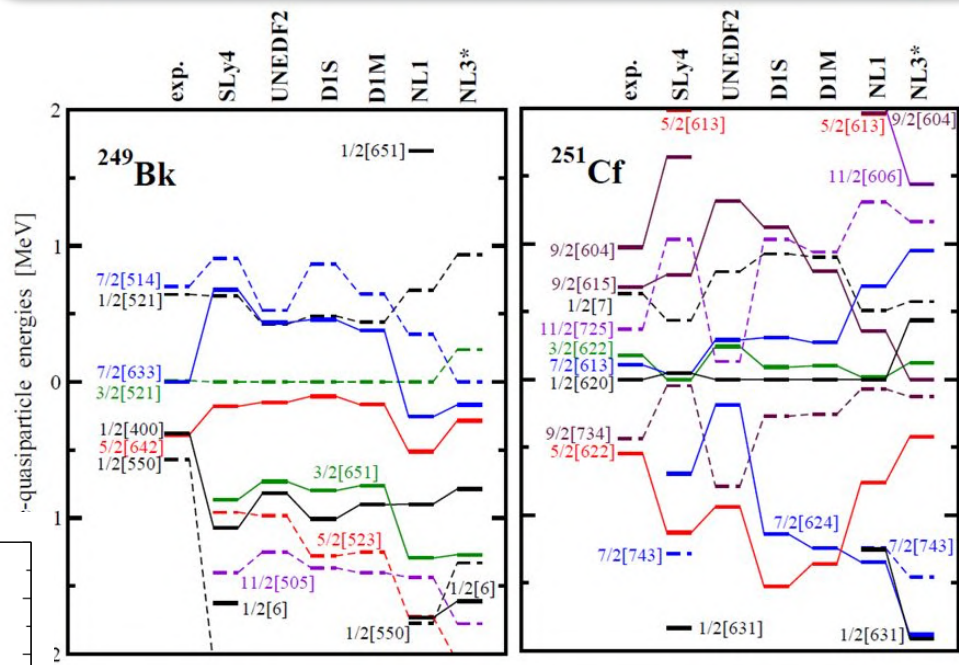
Systematic studies for ^{249}Bk and ^{251}Cf in the mean-field approximation:

$$^{250}\text{Cf}$$

$$\beta_2 = 0.29$$



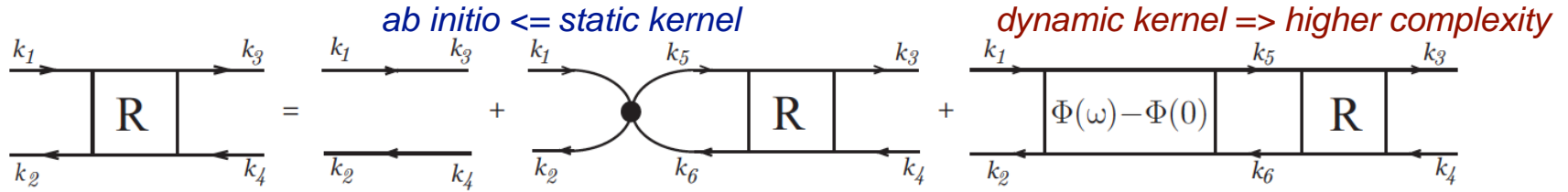
Deformed one-quasiparticle states: covariant and non-relativistic mean-field calculations vs experiment:



Beyond mean field: RHB+QVC calculations. Dominant fragments in ^{251}Cf and ^{249}Cf .

The spectroscopic factors are quenched even stronger than in spherical nuclei. Can this be measured?

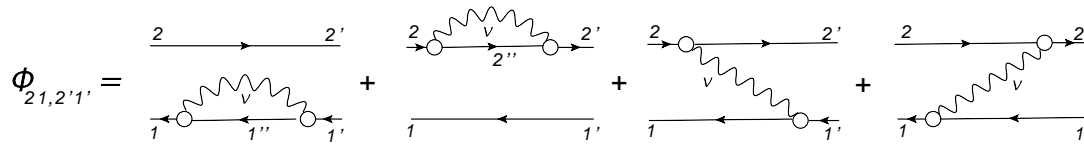
Nuclear response: toward a complete theory



Dyson-Bethe-Salpeter Equation:

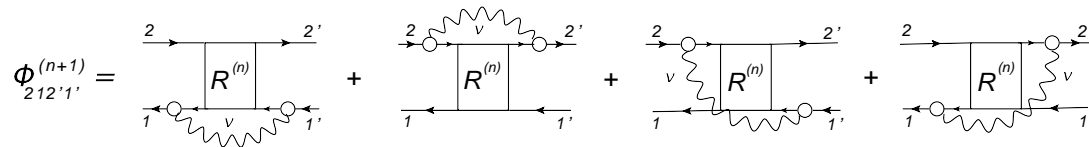
$$R(\omega) = R^0(\omega) + R^0(\omega) [V + \Phi(\omega) - \Phi(0)] R(\omega)$$

Conventional NFT



Subtraction for effective interactions (Tselyaev 2013)

Extended NFT:



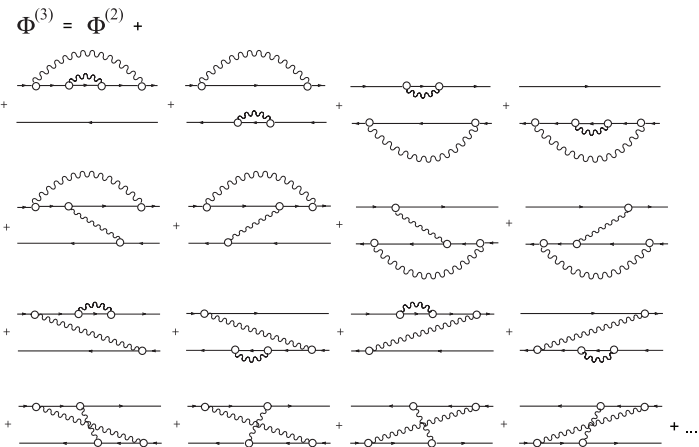
Generalized approach for the correlated propagators

n-th order: E.L. PRC 91, 034332 (2015)

Ab-initio formulation,

$\Phi^{(3)}$ implementation; 2q+2phonon correlations:

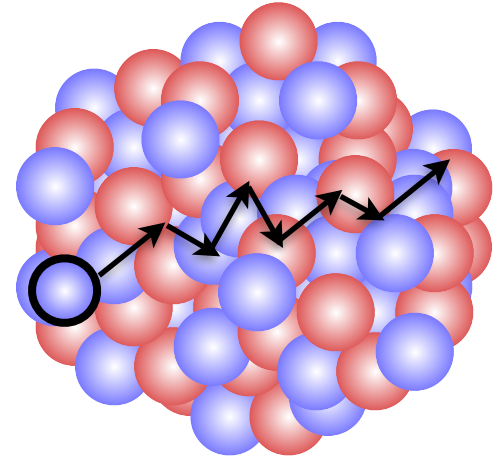
E.L., P. Schuck, PRC 100, 064320 (2019)



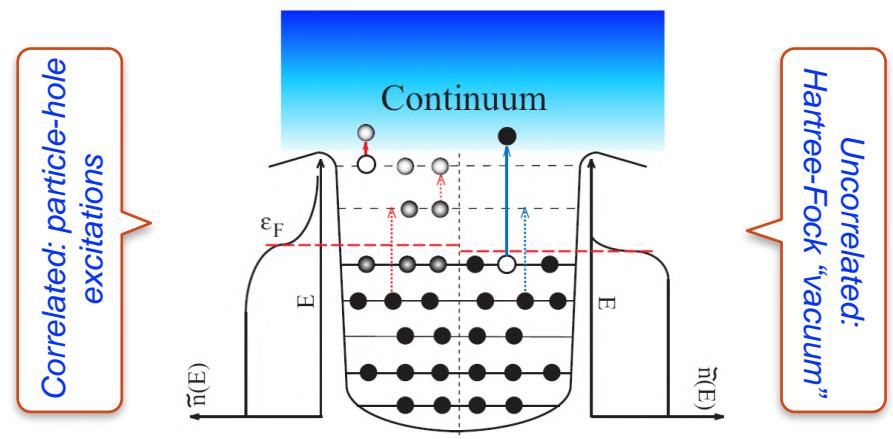
Individual (single-particle) and collective degrees of freedom

Single-particle

Single-particle in-medium propagation

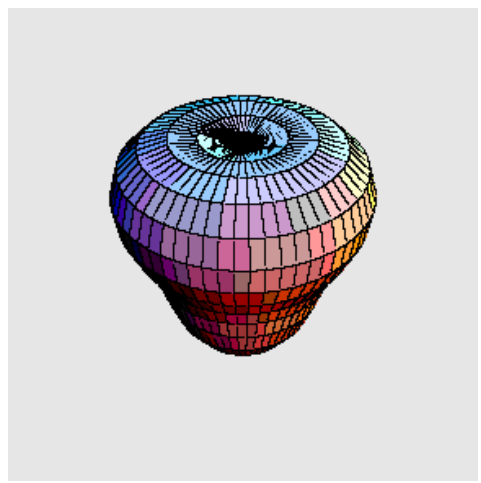


Single-particle energy spectrum

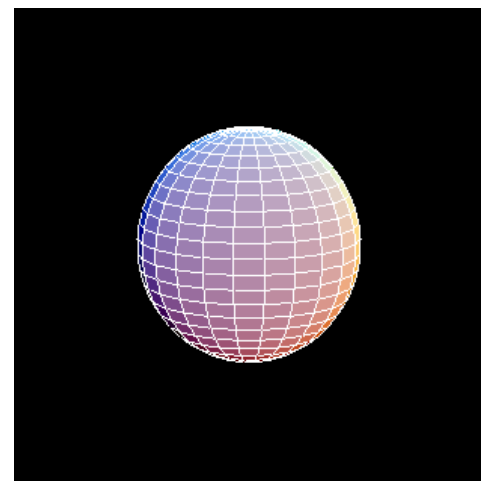


Collective

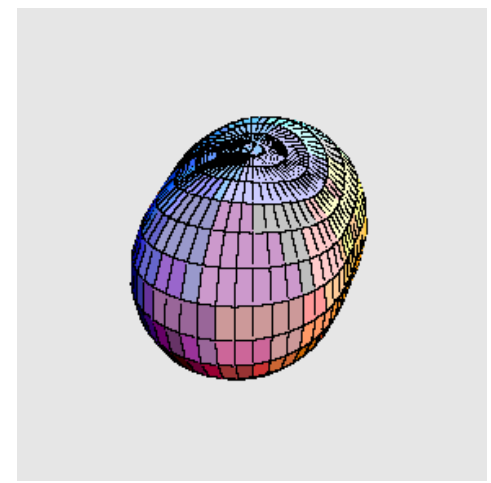
Octupole vibration



Quadrupole vibration



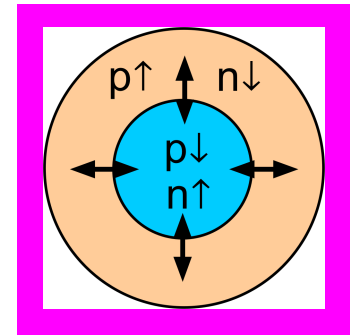
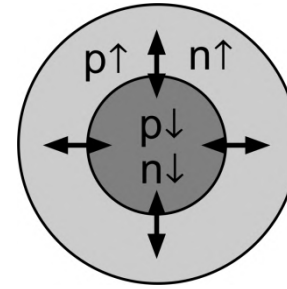
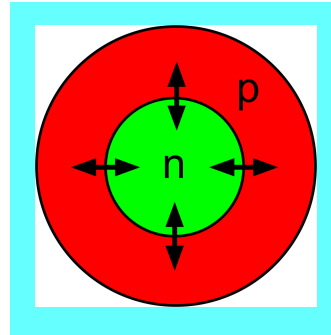
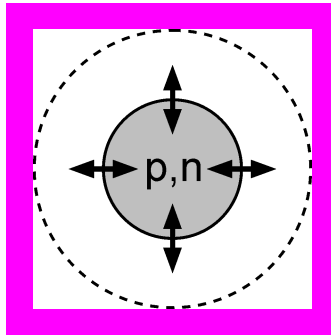
Rotation



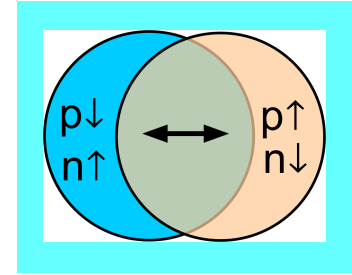
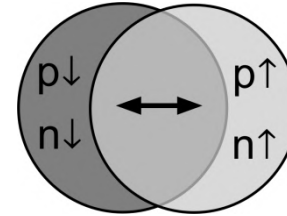
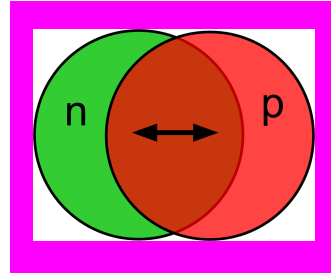
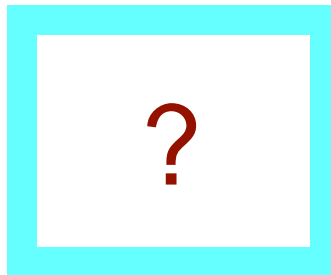
Nuclear excitation modes: classification

Gamow-Teller

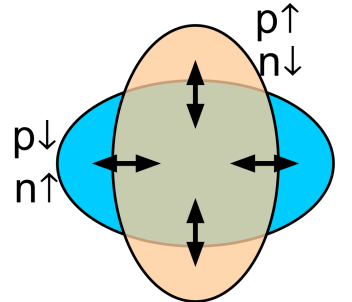
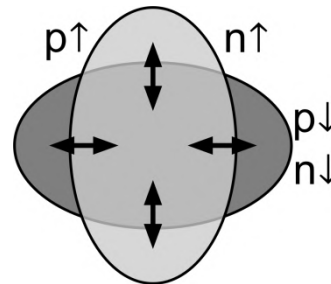
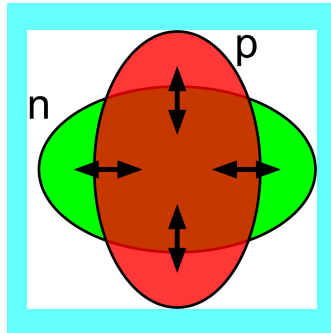
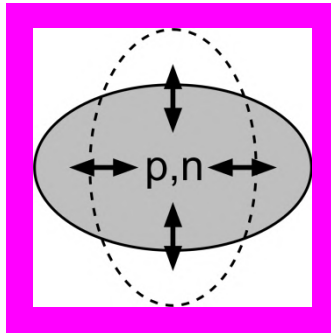
Monopole
 $\Delta L = 0$



Dipole
 $\Delta L = 1$



Quadrupole
 $\Delta L = 2$



$\Delta T = 0$
 $\Delta S = 0$

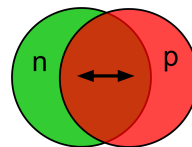
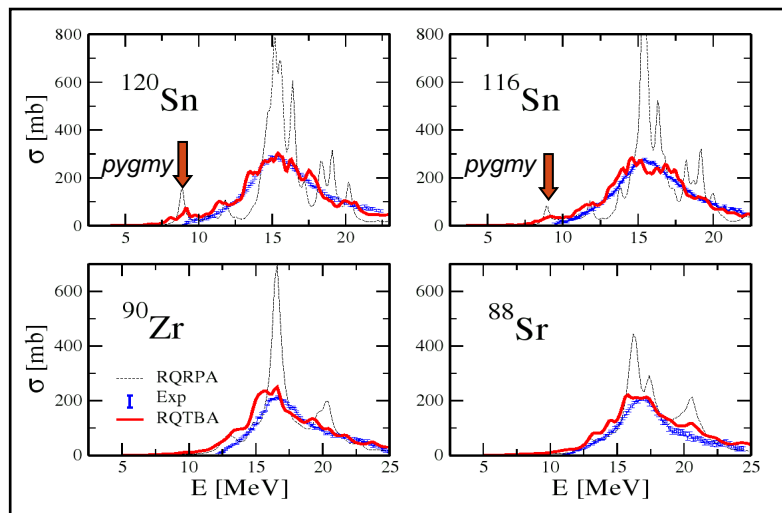
$\Delta T = 1$
 $\Delta S = 0$

$\Delta T = 0$
 $\Delta S = 1$

$\Delta T = 1$
 $\Delta S = 1$

Excitation modes in medium-mass and heavy nuclei within Relativistic Quasiparticle Time Blocking Approximation (RQTBA)

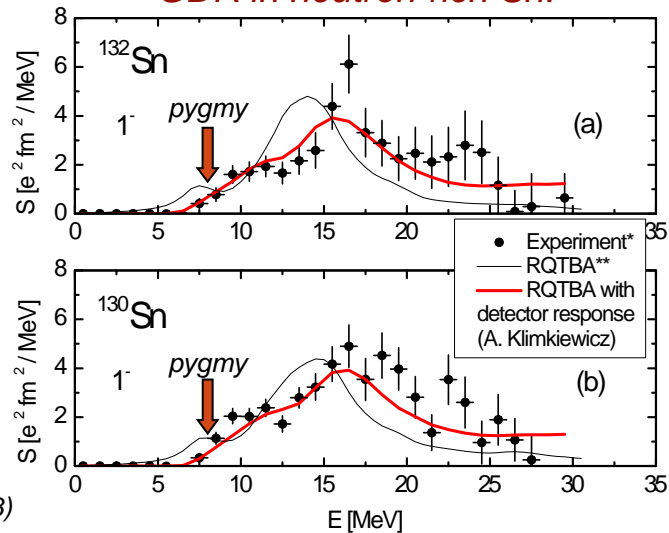
Giant dipole resonance (GDR) in stable nuclei:



Giant & pygmy dipole resonances

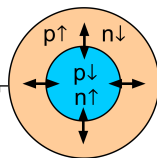
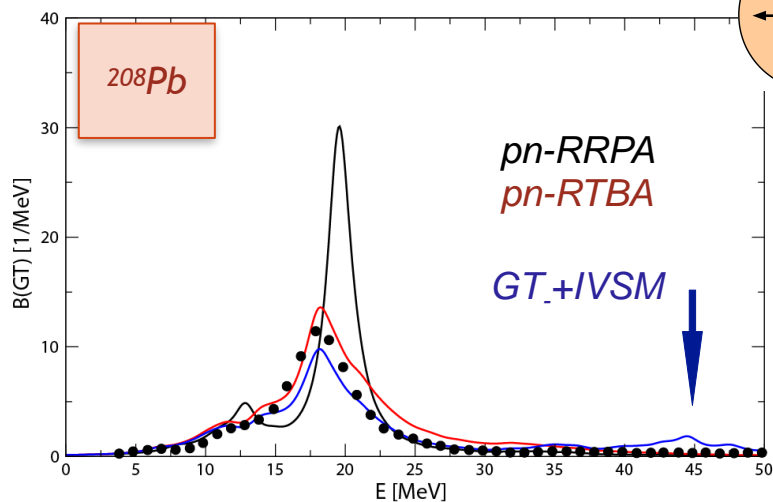
**E. L., P. Ring, and V. Tselyaev, Phys. Rev. C 78, 014312 (2008)

GDR in neutron-rich Sn:



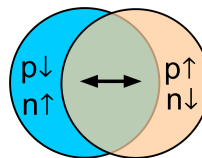
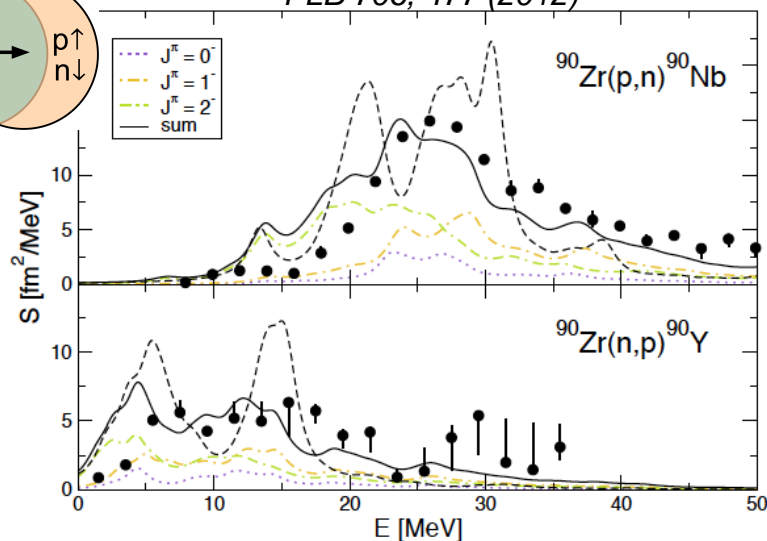
Gamow-Teller (with IV spin-monopole) resonance:

E.L., B.A. Brown, D.-L. Fang, T. Marketin, R.G.T. Zegers, PLB 730, 307 (2014)



Spin-Dipole resonance:

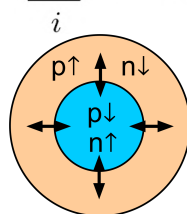
T. Marketin, E.L., D. Vretenar, P. Ring, PLB 706, 477 (2012)



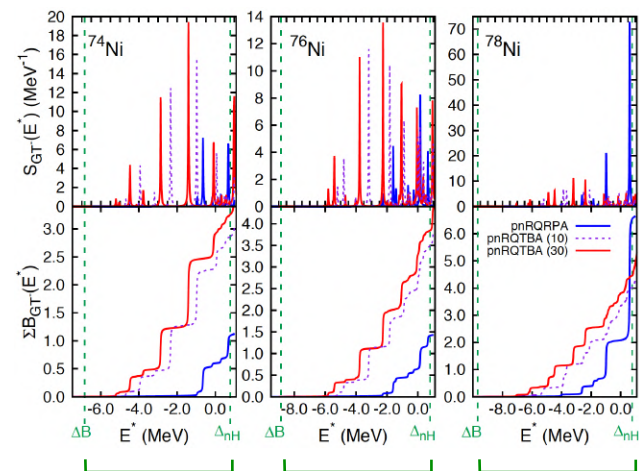
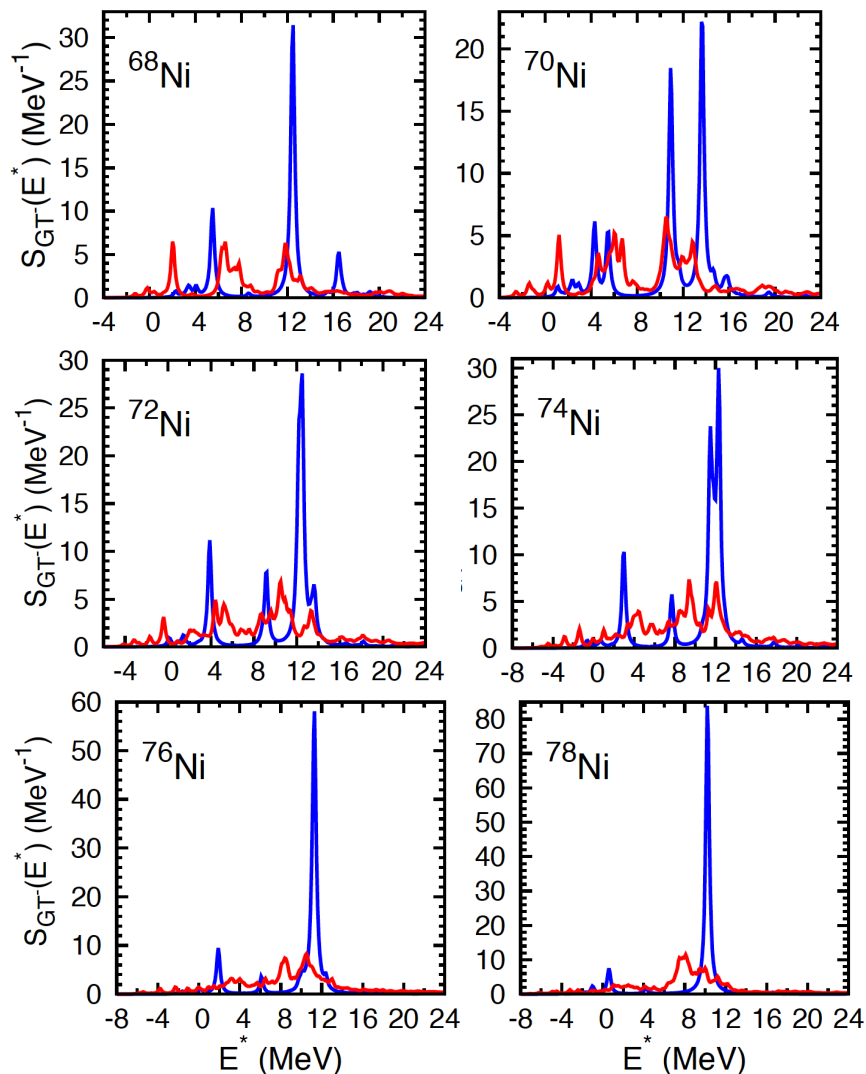
Spin-isospin excitations (Gamow-Teller resonance) 2q+phonon configurations in the dynamical kernel (pn-RQTBA)

Overall strength

$$P = \sum_i \sigma^{(i)} \tau_{\pm}^{(i)}$$



Low-energy part: Q_{β} window

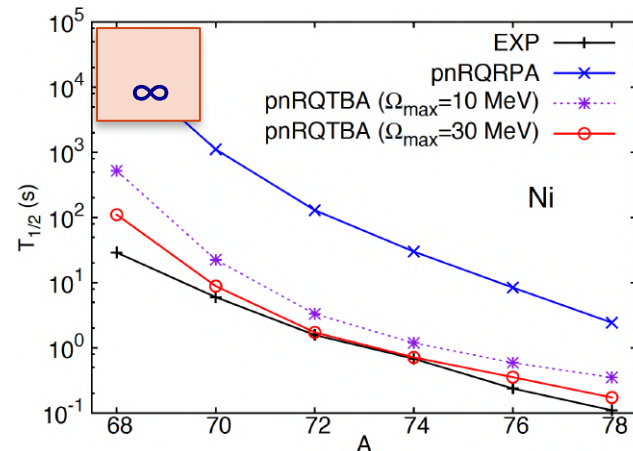


Q_{β}

Q_{β}

Q_{β}

$$\frac{1}{T_{1/2}} = \sum_m \lambda_{if}^m = D^{-1} g_A^2 \sum_m \int dE_e \left| \sum_{pn} \langle 1_{\lambda}^+ || \sigma \tau_{-} || 0^+ \rangle \right|^2 \frac{dn_m}{dE_e}$$



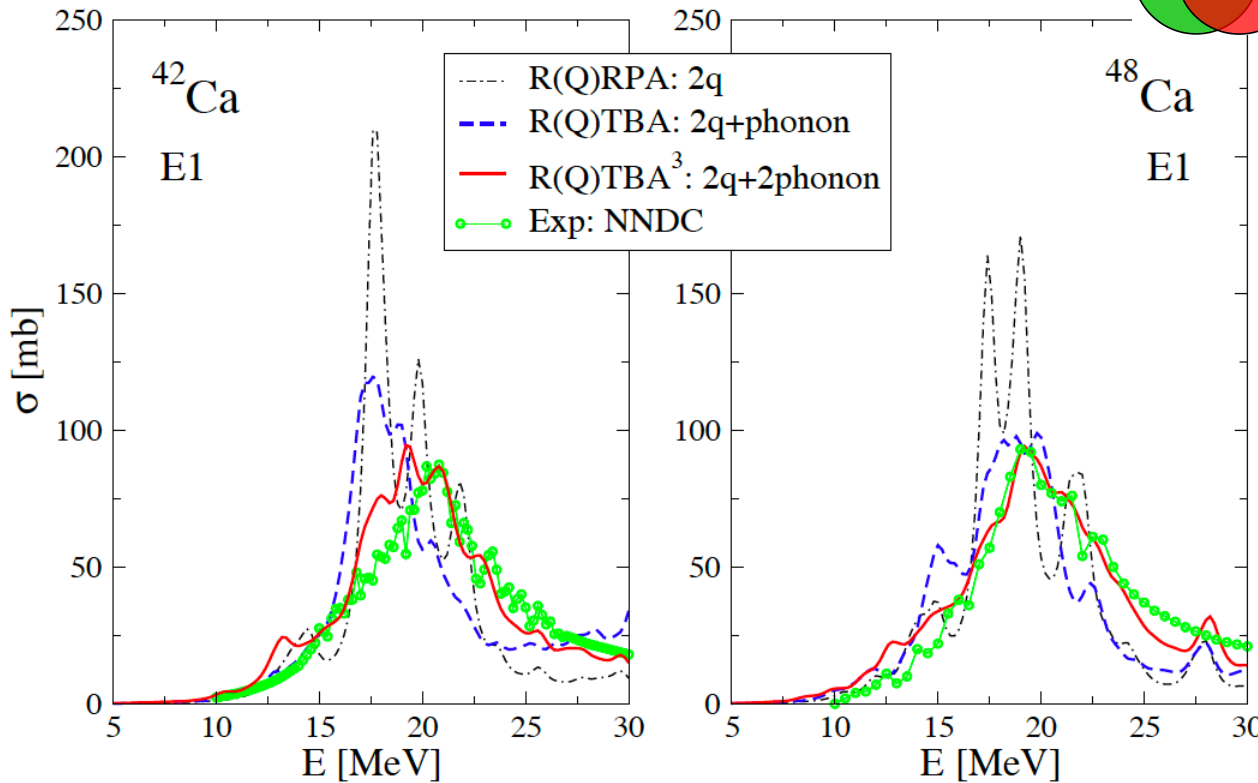
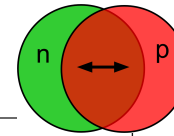
— pn -RQRPA
— pn -RQTBA

C. Robin, E.L.,
Eur. Phys. J. A 52, 205 (2016)

No fits, no artificial quenching,
no adjustable proton-neutron pairing

RQTBA³ with correlated 3p3h configurations: 2q+2phonon

Giant Dipole Resonance in Ca isotopes



• The new complex configurations 2q+2phonon included for the first time enforce fragmentation and spreading toward higher and lower energies, thus, modifying both giant and pygmy dipole resonances;

• Exp. Data: V.A. Erokhova et al., Bull. Rus. Acad. Phys. 67, 1636 (2003)

• RQTBA³ demonstrates an overall systematic improvement of the description of nuclear excited states heading toward spectroscopic accuracy without strong limitations on masses and excitation energies.

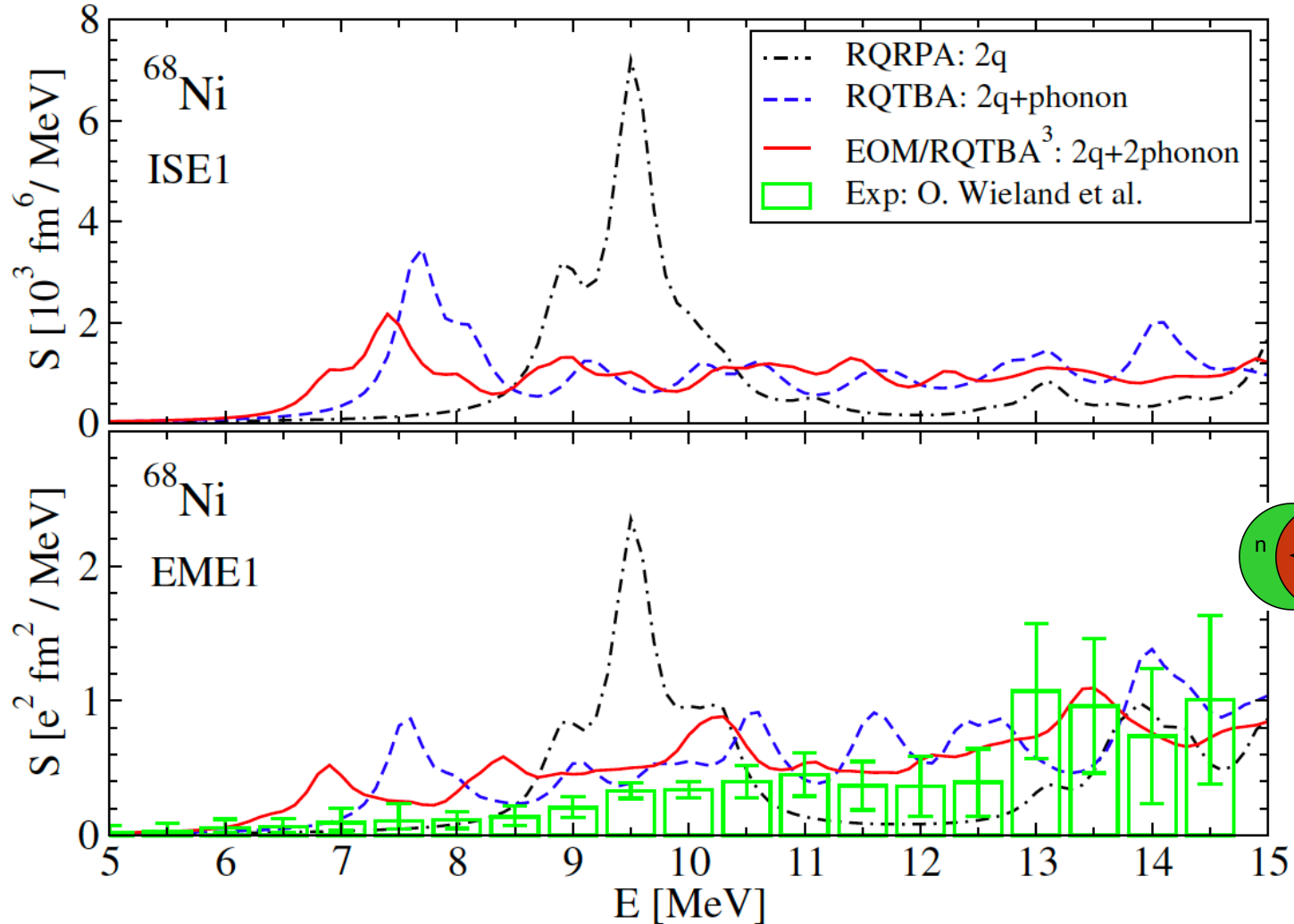
E.L., P. Schuck,
PRC 100, 064320 (2019)

Interaction kernel:
($n = 2$)

$$\Phi_{212'1'}^{(n+1)} = \begin{array}{c} \begin{array}{c} \xrightarrow{2} \\ \xrightarrow{1} \end{array} \left[\begin{array}{c} \xrightarrow{2'} \\ \xrightarrow{1'} \end{array} \right] \\ \begin{array}{c} \xrightarrow{2} \\ \xrightarrow{1} \end{array} \end{array} R^{(n)} \begin{array}{c} \xrightarrow{2'} \\ \xrightarrow{1'} \end{array} + \begin{array}{c} \begin{array}{c} \xrightarrow{2} \\ \xrightarrow{1} \end{array} \left[\begin{array}{c} \xrightarrow{2'} \\ \xrightarrow{1'} \end{array} \right] \\ \begin{array}{c} \xrightarrow{2} \\ \xrightarrow{1} \end{array} \end{array} R^{(n)} \begin{array}{c} \xrightarrow{2'} \\ \xrightarrow{1'} \end{array} + \begin{array}{c} \begin{array}{c} \xrightarrow{2} \\ \xrightarrow{1} \end{array} \left[\begin{array}{c} \xrightarrow{2'} \\ \xrightarrow{1'} \end{array} \right] \\ \begin{array}{c} \xrightarrow{2} \\ \xrightarrow{1} \end{array} \end{array} R^{(n)} \begin{array}{c} \xrightarrow{2'} \\ \xrightarrow{1'} \end{array} + \begin{array}{c} \begin{array}{c} \xrightarrow{2} \\ \xrightarrow{1} \end{array} \left[\begin{array}{c} \xrightarrow{2'} \\ \xrightarrow{1'} \end{array} \right] \\ \begin{array}{c} \xrightarrow{2} \\ \xrightarrow{1} \end{array} \end{array} R^{(n)} \begin{array}{c} \xrightarrow{2'} \\ \xrightarrow{1'} \end{array}$$

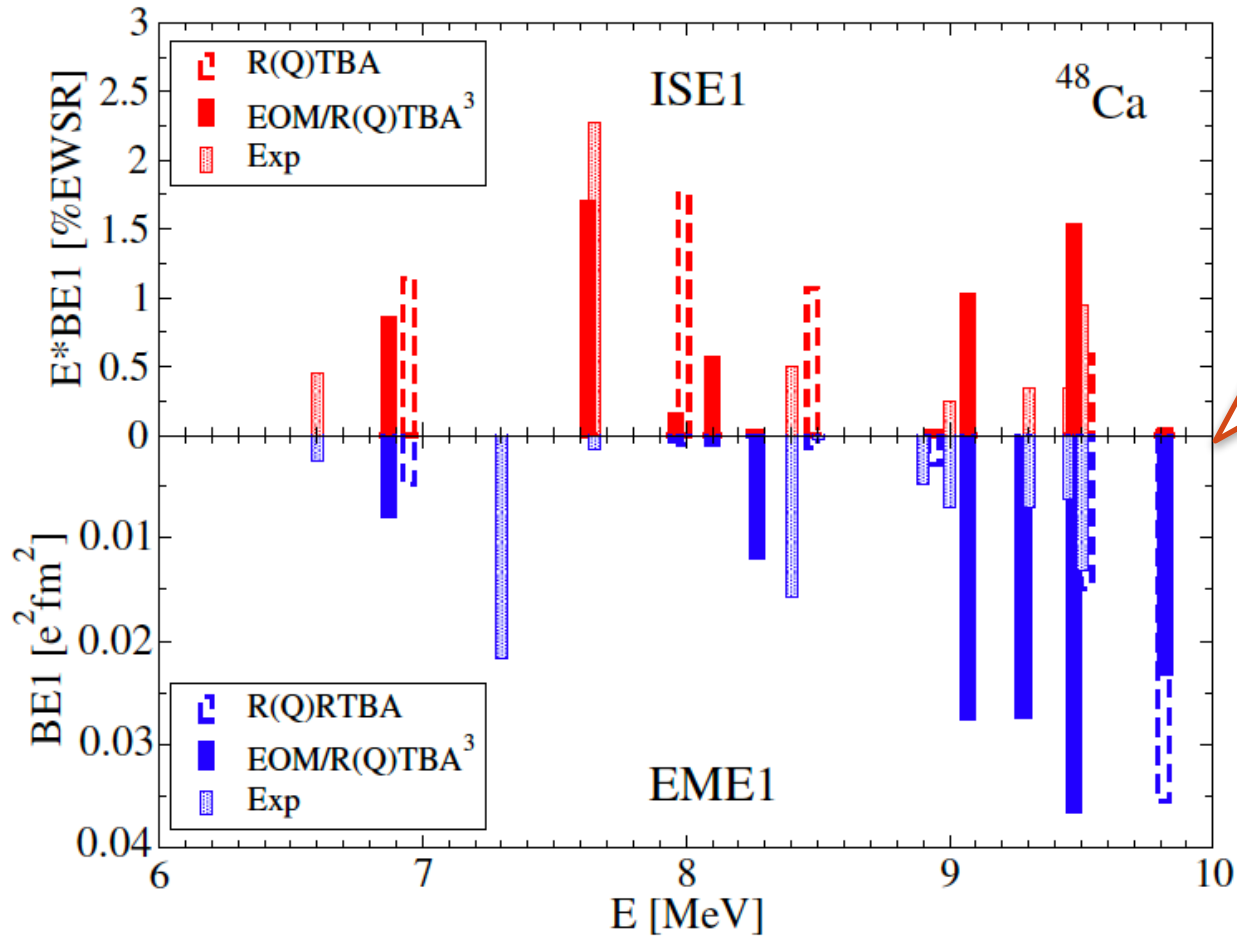
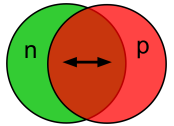
RQTBA³ with correlated 3p3h configurations: 2q+2phonon

Low-Energy dipole strength distribution: IS vs EM



RQTBA³ with correlated 3p3h configurations: 2q+2phonon

Low-energy dipole strength in ⁴⁸Ca: Electromagnetic vs Isoscalar



How / where do we continue?



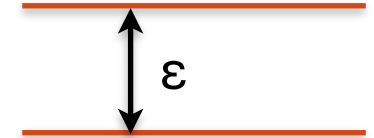
Are there theoretical limits on accuracy?

- *Higher-rank configurations = higher accuracy? Can we quantify this? How accurately we can describe the observed spectra, in principle?*
- *Spectroscopic accuracy in nuclear structure: experiment (laser spectroscopy [eV], nuclear resonance fluorescence [keV]) ... no standards for theory. ~100 keV?*
- *Chemical accuracy 1 kcal/mol = 0.043 eV is possible with the gold standard for quantum chemistry calculations, namely the canonical coupled cluster (CC) expansion truncated at the second order in the electronic excitation operator and including an approximate treatment of the triple excitations (CCSD(T), where S stands for single, D for double, and (T) for non-iterative triple) [P.J. Ollitrault et al, Phys. Rev. Res. 2, 043140, 2020]*
- *CCSD(T) includes up to (correlated) 3p3h configurations and scales as $O(N^7)$ with the number of degrees of freedom N of the model Hamiltonian.*
- *In nuclear structure, there are relatively rare calculations with (correlated) 3p3h configurations for medium-heavy nuclei (QPM, EOM/RQTBA³, CC). The results are still not ideal.*
- *Is the problem in the underlying strong “forces”, which are not weak and known with limited accuracy? Or the many-body methods? Likely both.*
- *Working with model (solvable) Hamiltonians allows one to solely focus on the many-body problem. Can be studied with quantum and hybrid algorithms on NISQ devices.*

Lipkin Hamiltonian on quantum computer

Two-level Lipkin (Meshkov-Glick), LMG, Hamiltonian:

$$\hat{H} = \epsilon \hat{J}_z - \frac{v}{2} \left(\hat{J}_+^2 + \hat{J}_-^2 \right) - \frac{w}{2} \left(\hat{J}_+ \hat{J}_- + \hat{J}_- \hat{J}_+ \right)$$



Quasispin operators:

$$\hat{J}_z = \frac{1}{2} \sum_{p=1}^N \left(\hat{a}_{p,+}^\dagger \hat{a}_{p,+} - \hat{a}_{p,-}^\dagger \hat{a}_{p,-} \right),$$

$$N = 2j + 1$$

$$\hat{J}_+ = \sum_{p=1}^N \hat{a}_{p,+}^\dagger \hat{a}_{p,-} \quad \text{and} \quad \hat{J}_- = \left(\hat{J}_+ \right)^\dagger$$

Excitation operator:

$$\hat{O}_n^\dagger = \sum_{\alpha} \sum_{\mu_{\alpha}} \left[X_{\mu_{\alpha}}^{\alpha}(n) \hat{K}_{\mu_{\alpha}}^{\alpha} - Y_{\mu_{\alpha}}^{\alpha}(n) \left(\hat{K}_{\mu_{\alpha}}^{\alpha} \right)^\dagger \right]$$

Configuration complexity:

$$\hat{K}_{\mu_1}^1 = a_i^\dagger a_{j'}$$

$$\hat{K}_{\mu_2}^2 = a_i^\dagger a_j^\dagger a_{j'} a_{i'}$$

...

The algorithm: Variational Quantum Eigensolver (VQE) + quantum EOM (qEOM)

- VQE: a minimal encoding scheme is found (“J-scheme”) and implemented, based on the symmetry of the LMG Hamiltonian. Yields an accurate ground state $|0\rangle$.
- qEOM generates efficiently the EOM matrix:

$$\begin{bmatrix} \mathcal{A} & \mathcal{B} \\ \mathcal{B}^* & \mathcal{A}^* \end{bmatrix} \begin{bmatrix} X^n \\ Y^n \end{bmatrix} = E_{0n} \begin{bmatrix} \mathcal{C} & \mathcal{D} \\ -\mathcal{D}^* & -\mathcal{C}^* \end{bmatrix} \begin{bmatrix} X^n \\ Y^n \end{bmatrix}$$

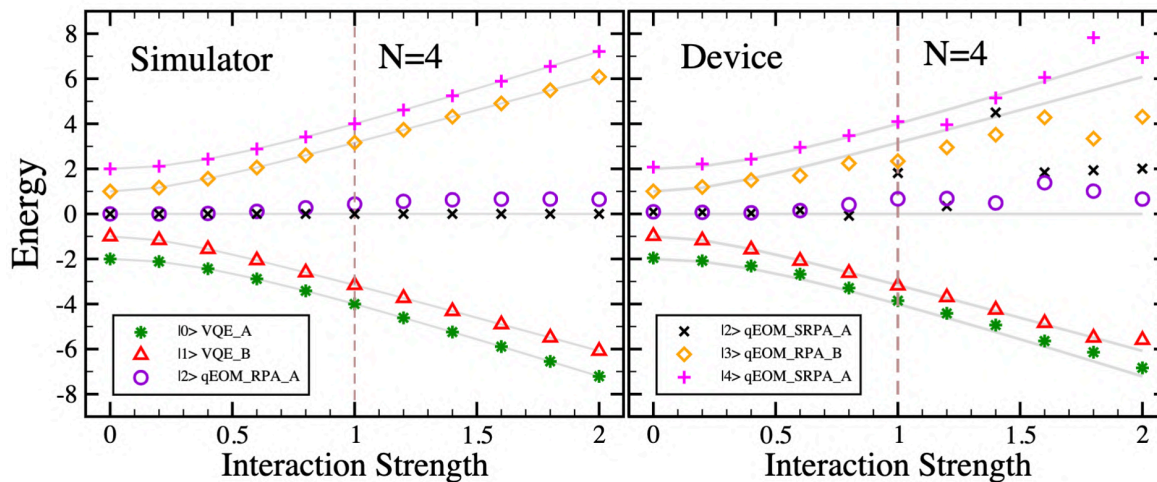
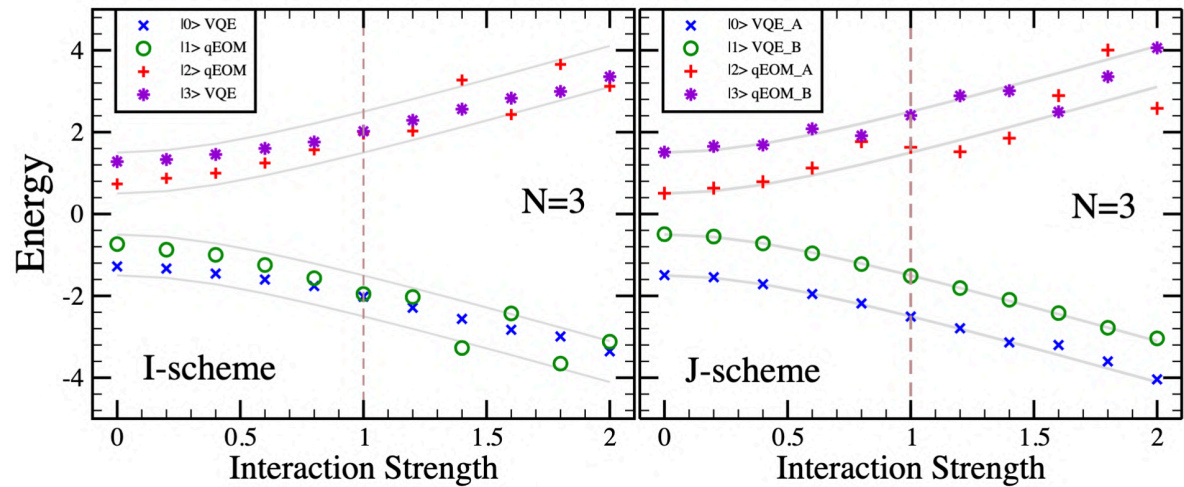
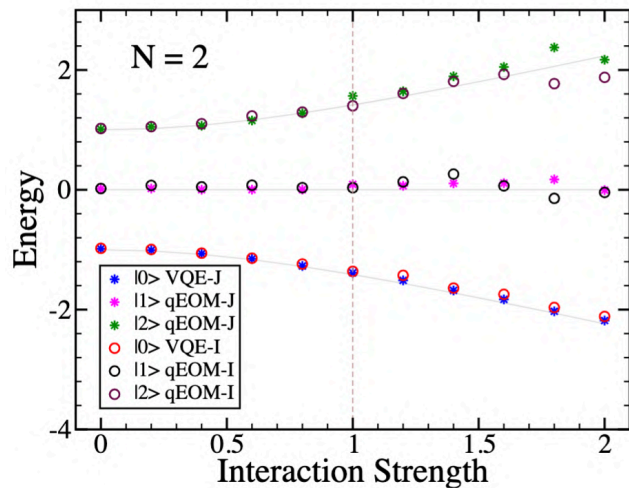
$$\mathcal{A}_{\mu_\alpha \nu_\beta} = \langle 0 | \left[\left(\hat{K}_{\mu_\alpha}^\alpha \right)^\dagger, \left[\hat{H}, \hat{K}_{\nu_\beta}^\beta \right] \right] | 0 \rangle$$

$$\mathcal{B}_{\mu_\alpha \nu_\beta} = - \langle 0 | \left[\left(\hat{K}_{\mu_\alpha}^\alpha \right)^\dagger, \left[\hat{H}, \left(\hat{K}_{\nu_\beta}^\beta \right)^\dagger \right] \right] | 0 \rangle$$

$$\mathcal{C}_{\mu_\alpha \nu_\beta} = \langle 0 | \left[\left(\hat{K}_{\mu_\alpha}^\alpha \right)^\dagger, \hat{K}_{\nu_\beta}^\beta \right] | 0 \rangle$$

$$\mathcal{D}_{\mu_\alpha \nu_\beta} = - \langle 0 | \left[\left(\hat{K}_{\mu_\alpha}^\alpha \right)^\dagger, \left(\hat{K}_{\nu_\beta}^\beta \right)^\dagger \right] | 0 \rangle.$$

Lipkin Hamiltonian on quantum computer: hardware results



Conventions:

- n_q = number of states
- N = number of particles
- $v = v/\epsilon$ effective interaction strength
- I-scheme:** individual spin basis, $n_q = 2^N$
- J-scheme:** total spin basis (coupled form), symmetry: $n_q = N/2 + 1$

Observations:

- Higher-rank excitation \sim higher accuracy
- Stronger coupling \sim lower accuracy
- More particles \sim lower accuracy
- Less qubits \sim higher accuracy

Finite-temperature response: the ph+phonon dynamical kernel

$$R_{12,1'2'}(t-t') = -i\langle \mathcal{T}(\bar{\psi}_1\psi_2)(t)(\bar{\psi}_{2'}\psi_{1'})(t') \rangle \rightarrow -i\langle \mathcal{T}(\bar{\psi}_1\psi_2)(t)(\bar{\psi}_{2'}\psi_{1'})(t') \rangle_T$$

$$\langle \dots \rangle \equiv \langle 0|\dots|0 \rangle \rightarrow \langle \dots \rangle_T \equiv \sum_n \exp\left(\frac{\Omega - E_n - \mu N}{T}\right) \langle n|\dots|n \rangle$$

averages



thermal averages

**Method: EOM
for Matsubara
Green's functions**



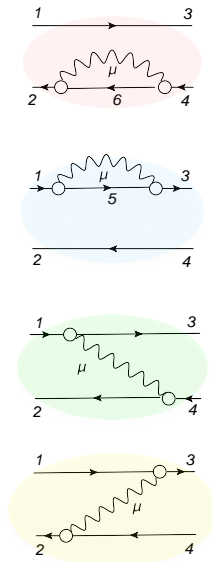
$$\mathcal{R}_{14,23}(\omega, T) = \tilde{\mathcal{R}}_{14,23}^0(\omega, T) + \sum_{1'2'3'4'} \tilde{\mathcal{R}}_{12',21'}^0(\omega, T) [\tilde{V}_{1'4',2'3'}(T) + \delta\Phi_{1'4',2'3'}(\omega, T)] \mathcal{R}_{3'4,4'3}(\omega, T)$$

$$\delta\Phi_{1'4',2'3'}(\omega, T) = \Phi_{1'4',2'3'}(\omega, T) - \Phi_{1'4',2'3'}(0, T)$$

$T > 0$:

$$\Phi_{14,23}^{(ph)}(\omega, T) = \frac{1}{n_{43}(T)} \sum_{\mu; \eta_{\mu} = \pm 1} \eta_{\mu} \left[\delta_{13} \sum_6 \gamma_{\mu;62}^{\eta_{\mu}} \gamma_{\mu;64}^{\eta_{\mu}*} \times \frac{(N(\eta_{\mu}\Omega_{\mu}) + n_6(T))(n(\varepsilon_6 - \eta_{\mu}\Omega_{\mu}, T) - n_1(T))}{\omega - \varepsilon_1 + \varepsilon_6 - \eta_{\mu}\Omega_{\mu}} + \delta_{24} \sum_5 \gamma_{\mu;15}^{\eta_{\mu}} \gamma_{\mu;35}^{\eta_{\mu}*} \times \frac{(N(\eta_{\mu}\Omega_{\mu}) + n_2(T))(n(\varepsilon_2 - \eta_{\mu}\Omega_{\mu}, T) - n_5(T))}{\omega - \varepsilon_5 + \varepsilon_2 - \eta_{\mu}\Omega_{\mu}} - \gamma_{\mu;13}^{\eta_{\mu}} \gamma_{\mu;24}^{\eta_{\mu}*} \times \frac{(N(\eta_{\mu}\Omega_{\mu}) + n_2(T))(n(\varepsilon_2 - \eta_{\mu}\Omega_{\mu}, T) - n_3(T))}{\omega - \varepsilon_3 + \varepsilon_2 - \eta_{\mu}\Omega_{\mu}} - \gamma_{\mu;31}^{\eta_{\mu}*} \gamma_{\mu;42}^{\eta_{\mu}} \times \frac{(N(\eta_{\mu}\Omega_{\mu}) + n_4(T))(n(\varepsilon_4 - \eta_{\mu}\Omega_{\mu}, T) - n_1(T))}{\omega - \varepsilon_1 + \varepsilon_4 - \eta_{\mu}\Omega_{\mu}} \right],$$

1p1h+phonon dynamical kernel:



$T = 0$:

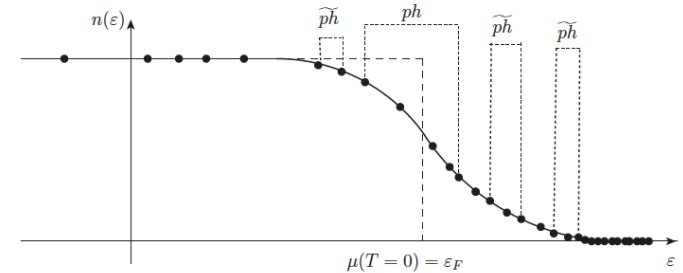
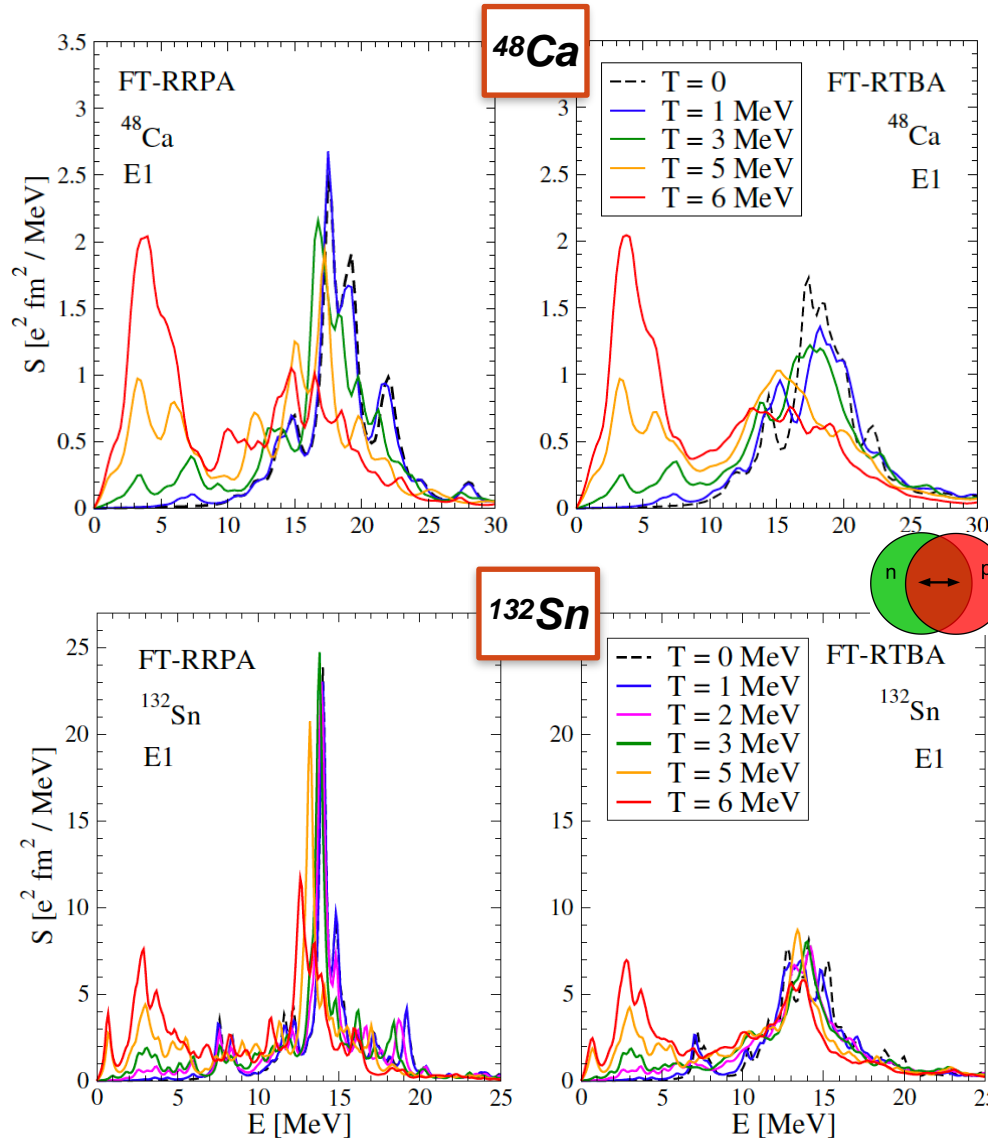
$$\Phi_{14,23}^{(ph,ph)}(\omega) = \sum_{\mu} \times \left[\delta_{13} \sum_6 \frac{\gamma_{62}^{\mu} \gamma_{64}^{\mu*}}{\omega - \varepsilon_1 + \varepsilon_6 - \Omega_{\mu}} + \delta_{24} \sum_5 \frac{\gamma_{15}^{\mu} \gamma_{35}^{\mu*}}{\omega - \varepsilon_5 + \varepsilon_2 - \Omega_{\mu}} - \frac{\gamma_{13}^{\mu} \gamma_{24}^{\mu*}}{\omega - \varepsilon_3 + \varepsilon_2 - \Omega_{\mu}} - \frac{\gamma_{31}^{\mu*} \gamma_{42}^{\mu}}{\omega - \varepsilon_1 + \varepsilon_4 - \Omega_{\mu}} \right]$$

Dipole Strength at $T > 0$: ^{48}Ca and ^{132}Sn

Static only (FT-RRPA)

Static + dynamic (FT-RTBA)

Thermal unblocking:



0th approximation:
Uncorrelated propagator $\tilde{R}_{14,23}^0(\omega) = \delta_{13}\delta_{24} \frac{n_2 - n_1}{\omega - \epsilon_1 + \epsilon_2}$

- New transitions due to the thermal unblocking effects
- More collective and non-collective modes contribute to the PVC self-energy (~400 modes at $T=5-6$ MeV)
- Broadening of the resulting GDR spectrum
- Development of the low-energy part => a feedback to GDR

- The spurious translation mode is properly decoupled as the mean field is modified consistently
- The role of the new terms in the Φ amplitude increases with temperature
- The role of dynamical correlations and fragmentation remain significant in the high-energy part

E.L., H. Wibowo, Phys. Rev. Lett. 121, 082501 (2018)

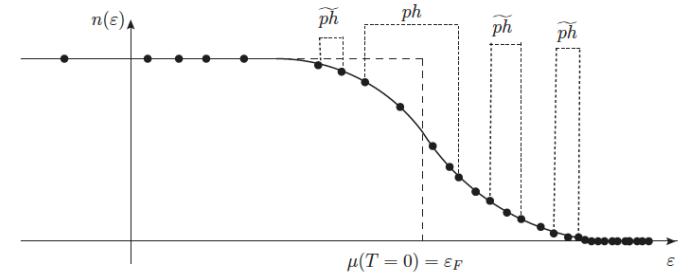
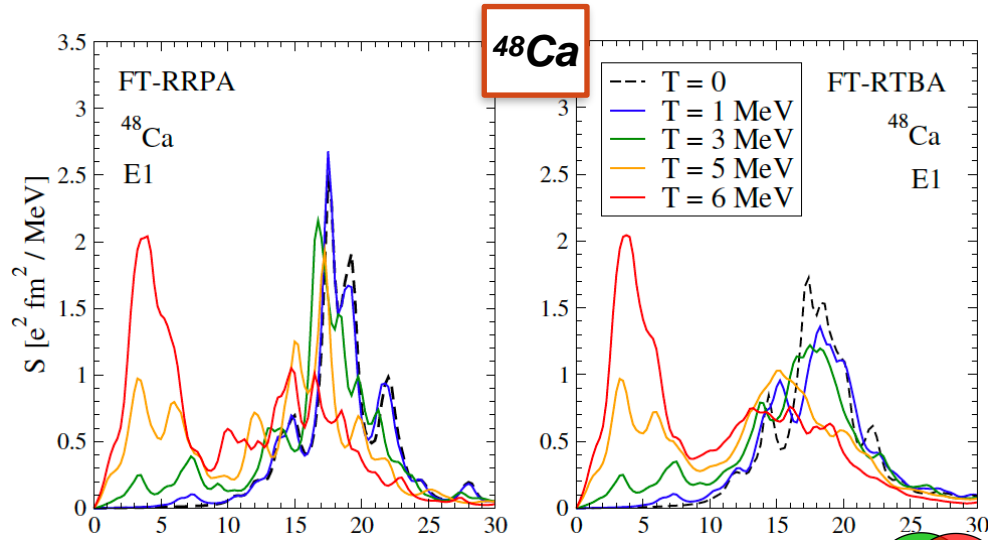
H. Wibowo, E.L., Phys. Rev. C 100, 024307 (2019)

Dipole Strength at $T > 0$: ^{48}Ca and ^{132}Sn

Static only (FT-RRPA)

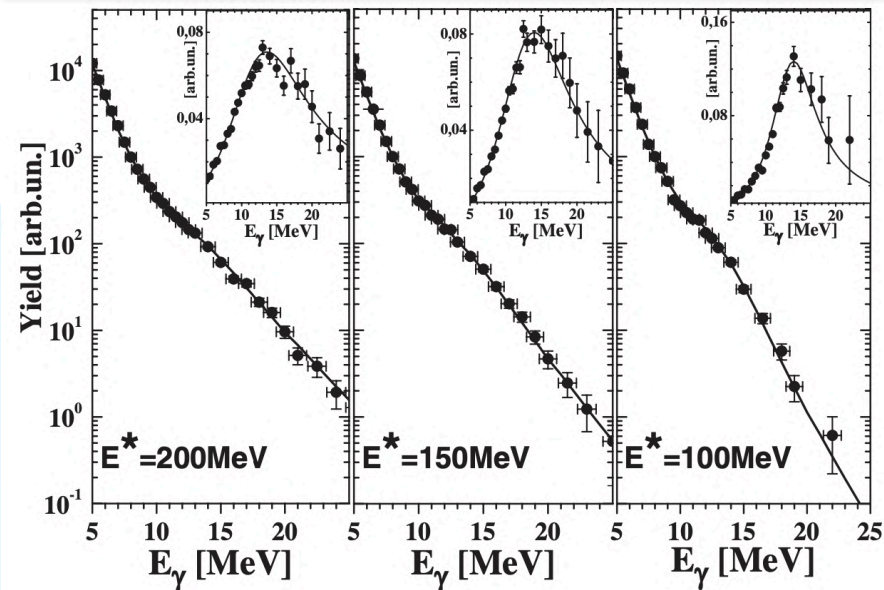
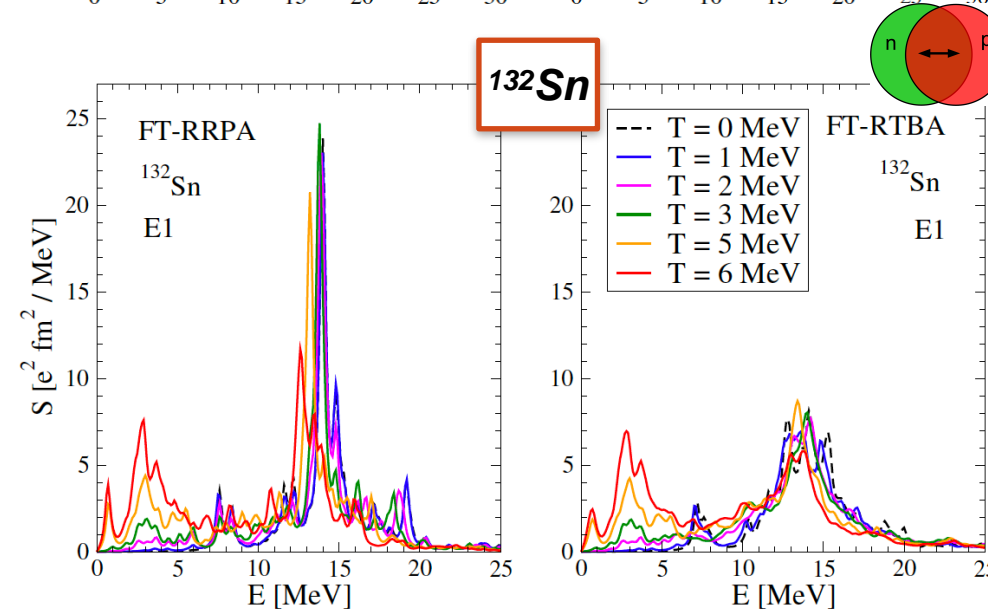
Static + dynamic (FT-RTBA)

Thermal unblocking:



0th approximation:
Uncorrelated propagator $\tilde{R}_{14,23}^0(\omega) = \delta_{13}\delta_{24} \frac{n_2 - n_1}{\omega - \epsilon_1 + \epsilon_2}$

O. Wieland et al., PRL **97**, 012501 (2006):
GDR in ^{132}Ce



The role of the exponential factor: low-energy strength

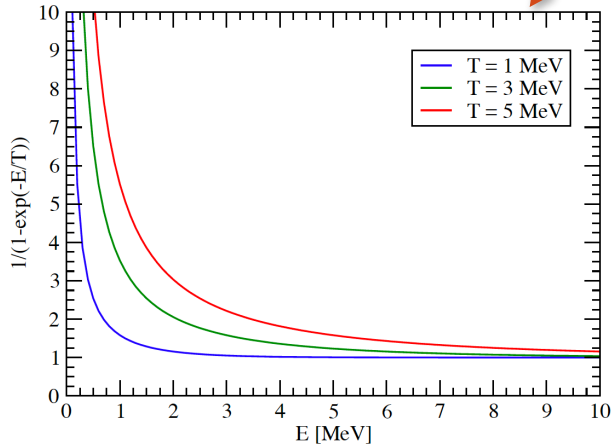
$$S(E, T) = -\frac{1}{\pi} \lim_{\Delta \rightarrow +0} \text{Im} \langle V^{0\dagger} \mathcal{R}(E + i\Delta, T) V^0 \rangle$$

The final strength function at $T > 0$:

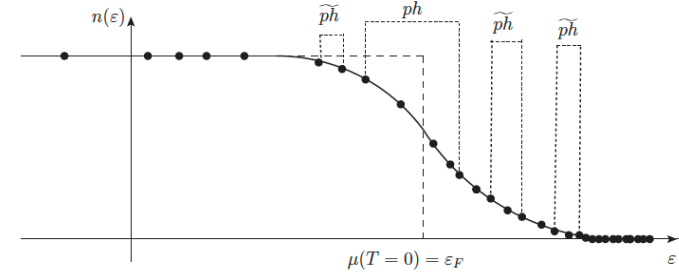
$$\tilde{S}(E) = \frac{1}{1 - e^{-E/T}} S(E)$$

$$\lim_{E \rightarrow 0} S(E, T) = 0$$

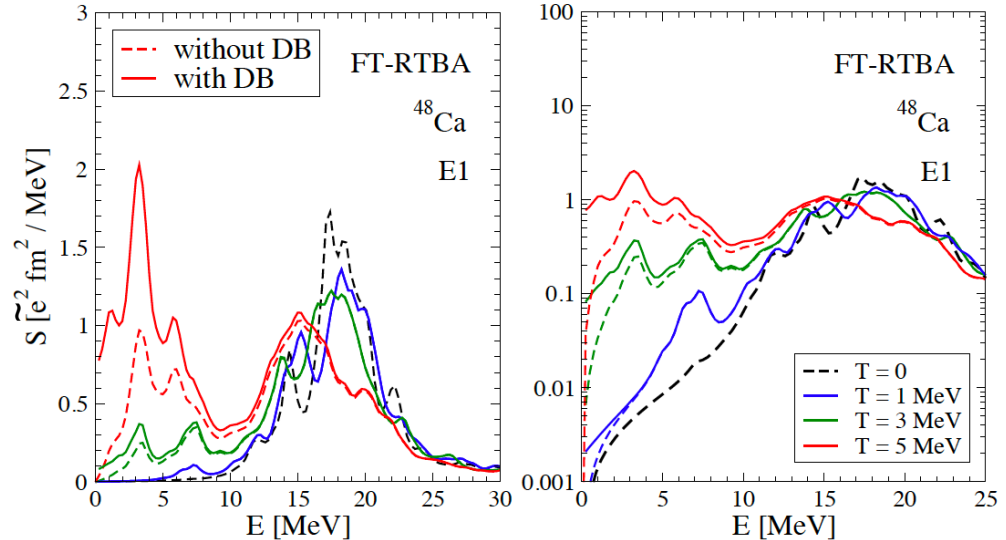
The **generic** exponential factor:



Thermal unblocking:



Dipole strength: absorption at $T > 0$:



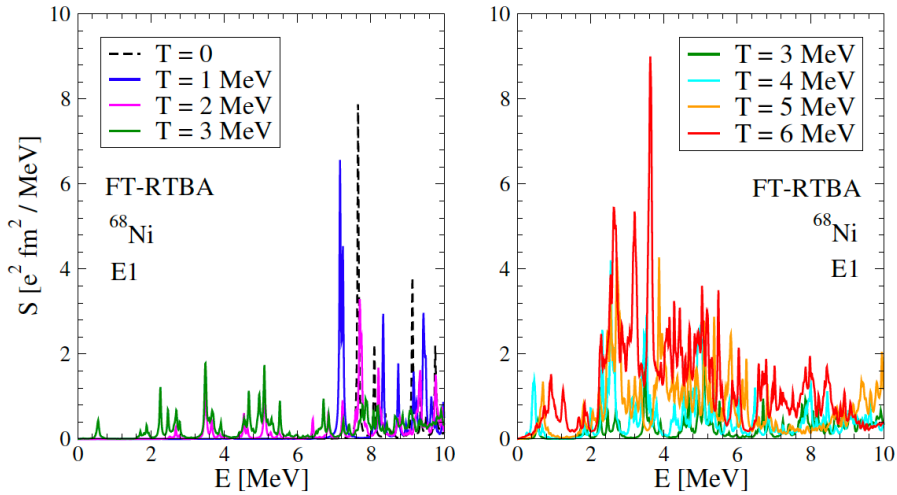
• The exponential factor brings an additional enhancement in $E < T$ energy region and provides the finite zero-energy limit of the strength (regardless its spin-parity)

E.L., H. Wibowo, *Phys. Rev. Lett.* 121, 082501 (2018)

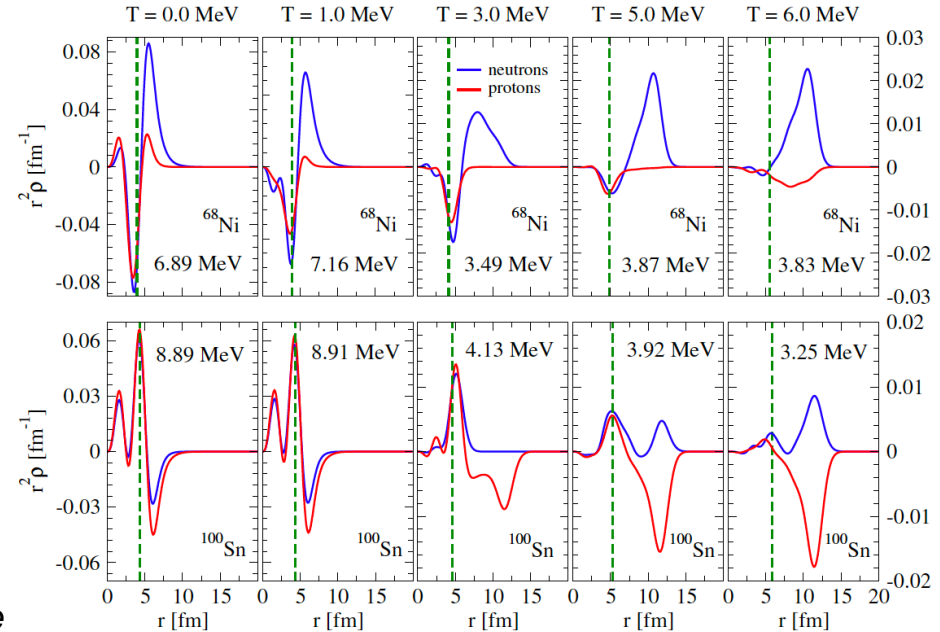
H. Wibowo, E.L., *Phys. Rev. C* 100, 024307 (2019)

Evolution of the pygmy dipole resonance (PDR) at $T > 0$

Low-energy strength distribution in ^{68}Ni

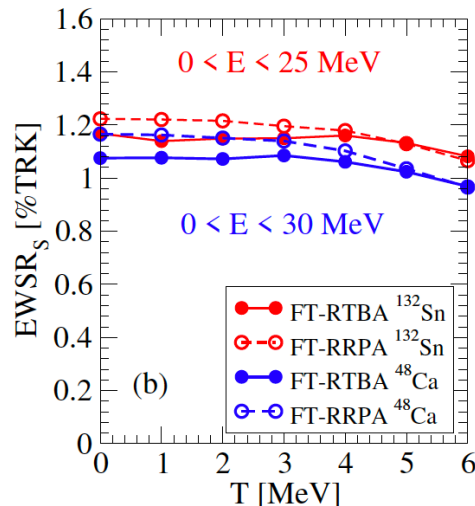
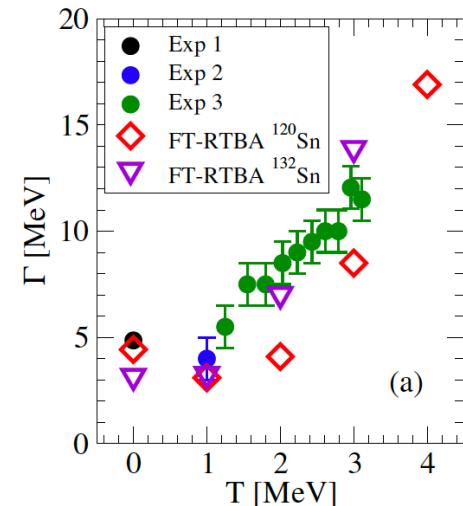


Transition density for the low-energy peak in ^{68}Ni , ^{100}Sn



GDR's width

Energy-weighted sum rule

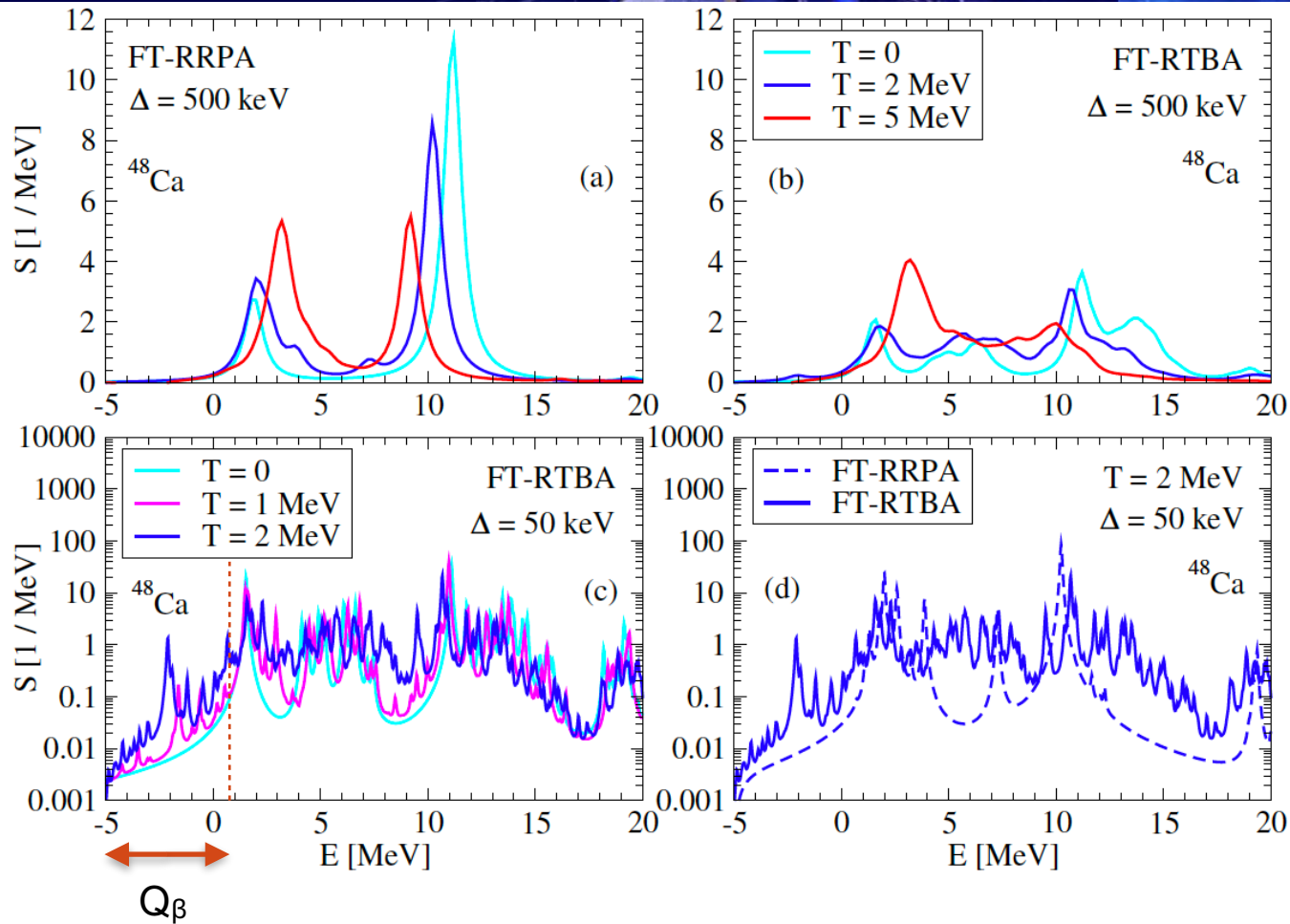


- The low-energy peak (PDR) gains the strength from the GDR with the temperature growth: $EWSR \sim \text{const}$
- The total width $\Gamma \sim T^2$ (as in the Landau theory); shape fluctuations are missing for $T \sim 2-3$ MeV
- The PDR develops a new type of collectivity originated from the thermal unblocking
- The same happens with other low-lying modes ($2+$, $3-$, ...) \Rightarrow strong PVC \Rightarrow "destruction" of the GDR at high temperatures

E.L., H. Wibowo, *Phys. Rev. Lett.* 121, 082501 (2018).

H. Wibowo, E.L., *Phys. Rev. C* 100, 024307 (2019).

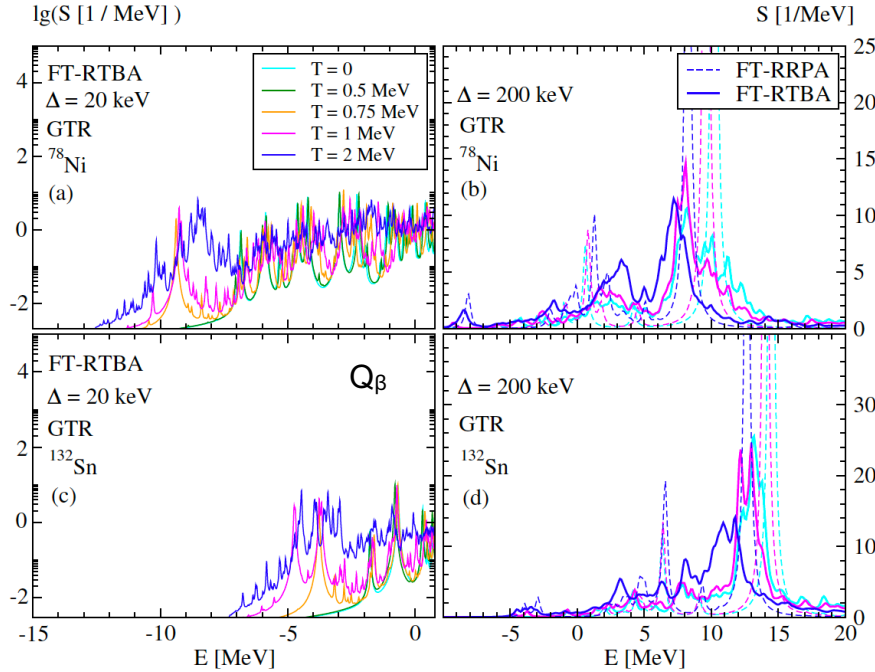
Temperature dependence of the Gamow-Teller Resonance (GTR): the case of ^{48}Ca



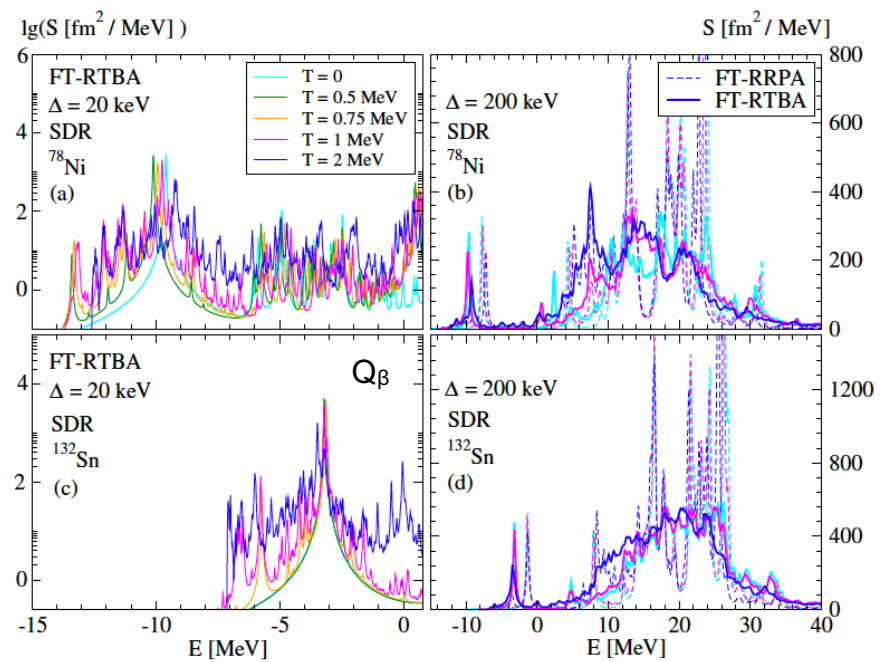
- The GTR shows a stronger sensitivity to temperature than the non-charge-exchange GDR.
- The strength gets “pumped” into the low-energy peak with the temperature increase.
- New states appear in the lowest-energy sector due to the thermal unblocking => **beta instability enhancement, thermally-induced beta decay**
- PVC fragmentation effects remain strong at $T > 0$.

Spin-Isospin response and beta decay in hot stellar environments

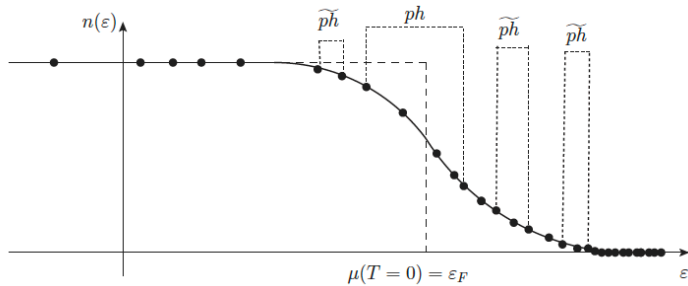
Gamow-Teller GT_- response of ^{78}Ni and ^{132}Sn



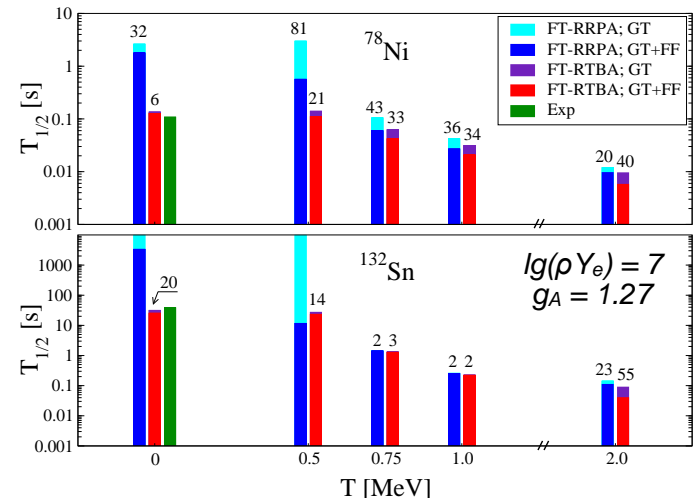
Spin Dipole response of ^{78}Ni and ^{132}Sn



Thermal unblocking mechanism:



Beta decay half-lives in a hot stellar environment



E. Litvinova, H. Wibowo, *Phys. Rev. Lett.* 121, 082501 (2018)

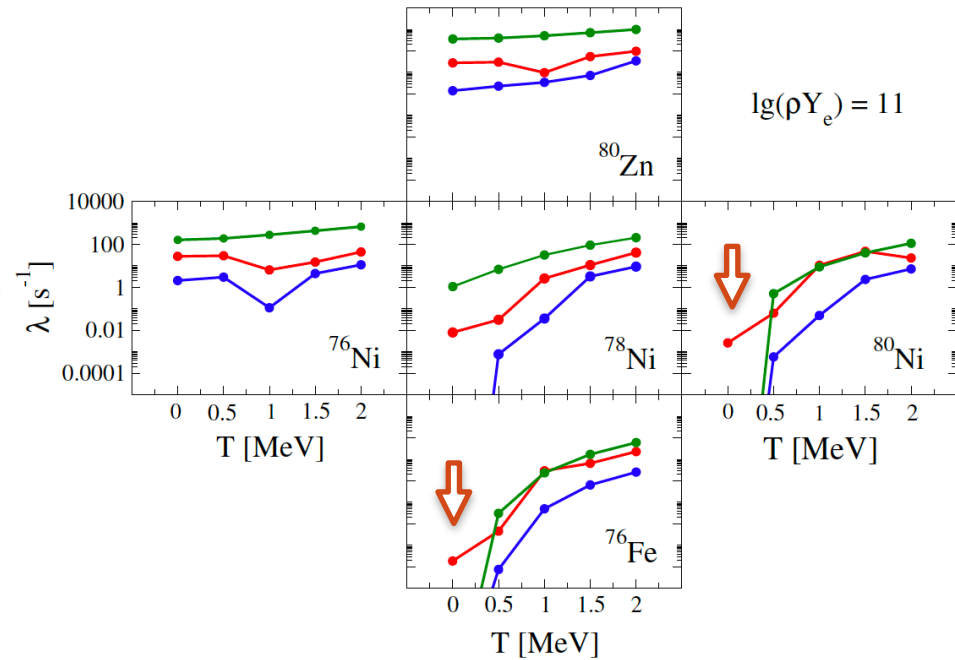
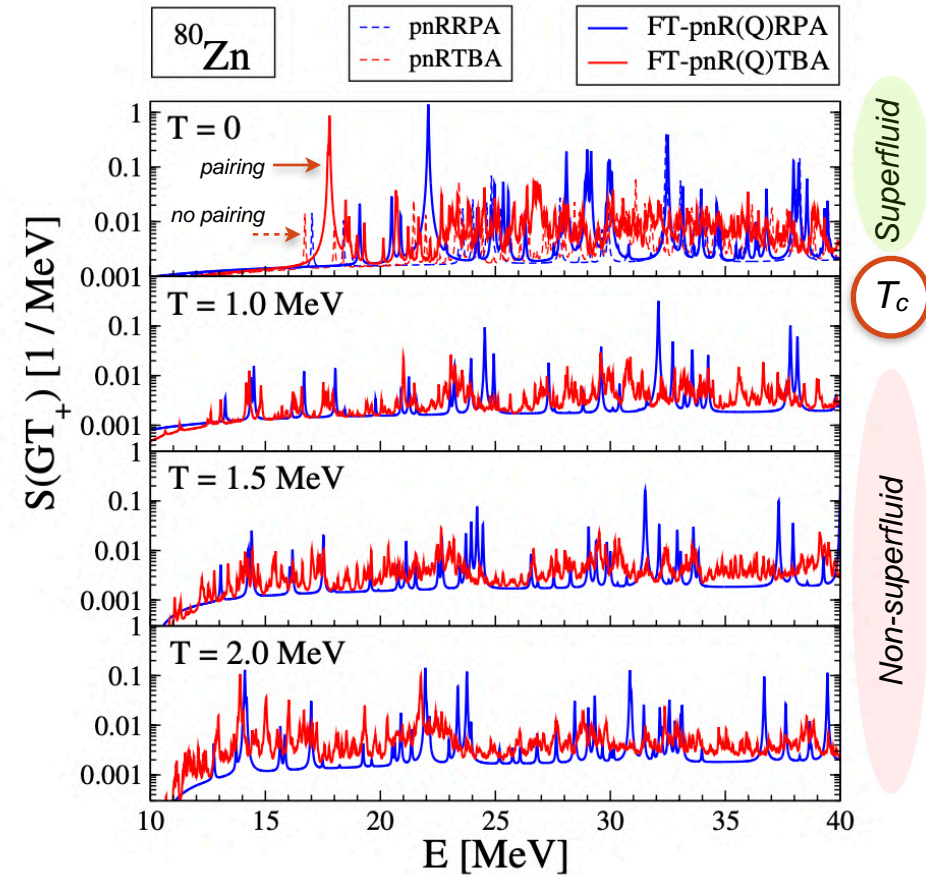
H. Wibowo, E. Litvinova, *Phys. Rev. C* 100, 024307 (2019)

E. Litvinova, C. Robin, H. Wibowo, *Phys. Lett. B* 800, 135134 (2020)

GT+ response and electron capture (EC) rates at $T > 0$: the neighborhood of ^{78}Ni

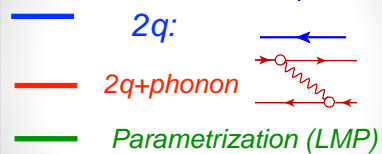
GT+ response

Electron capture rates around ^{78}Ni



Interplay of superfluidity and collective effects in core-collapse supernovae:

- Amplifies the EC rates and, consequently,
- Reduces the electron-to-baryon ratio leading to lower pressure
- Promotes the gravitational collapse
- Increases the neutrino flux and effective cooling
- Allows heavy nuclei to survive the collapse



E.L., C. Robin, H. Wibowo, PLB 800, 135134 (2020)

E.L., P. Schuck, PRC 104, 044330 (2021)

E.L., C. Robin, PRC 103, 024326 (2021)

Formalism at $T > 0$: the pairing channel

Averages redefined:

$$G_{12,1'2'}(t - t') = -i \langle \mathcal{T}(\psi_1 \psi_2)(t) (\bar{\psi}_{2'} \bar{\psi}_{1'})(t') \rangle \rightarrow -i \langle \mathcal{T}(\psi_1 \psi_2)(t) (\bar{\psi}_{2'} \bar{\psi}_{1'})(t') \rangle_T$$

Grand Canonical average: $\langle \dots \rangle \equiv \langle 0 | \dots | 0 \rangle \rightarrow \langle \dots \rangle_T \equiv \sum_n \exp\left(\frac{\Omega - E_n - \mu N}{T}\right) \langle n | \dots | n \rangle$

Matsubara imaginary-time formalism: temperature-dependent dynamical kernel

Direct:

$$\begin{aligned} \mathcal{K}_{121'2'}^{(r;11)}(\omega_n) &= - \sum_{\nu'\nu''} w_{\nu'} w_{\nu''} \\ &\times \left[\sum_{\nu\mu} \frac{\Theta_{121'2'}^{\mu\nu;\nu'\nu''(+)} }{i\omega_n - \omega_{\nu\nu'} - \omega_{\mu\nu''}^{(++)}} (e^{-(\omega_{\nu\nu'} + \omega_{\mu\nu''}^{(++)})/T} - 1) \right. \\ &\left. - \sum_{\nu\kappa} \frac{\Theta_{121'2'}^{\kappa\nu;\nu'\nu''(-)} }{i\omega_n + \omega_{\nu\nu'} + \omega_{\kappa\nu''}^{(--)}} (e^{-(\omega_{\nu\nu'} + \omega_{\kappa\nu''}^{(--)})/T} - 1) \right] \end{aligned}$$

Exchange:

$$\begin{aligned} \mathcal{K}_{121'2'}^{(r;12)}(\omega_n) &= \sum_{\nu'\nu''} w_{\nu'} w_{\nu''} \\ &\times \left[\sum_{\nu\mu} \frac{\Sigma_{121'2'}^{\mu\nu;\nu'\nu''(+)} }{i\omega_n - \omega_{\nu\nu'} - \omega_{\mu\nu''}^{(++)}} (e^{-(\omega_{\nu\nu'} + \omega_{\mu\nu''}^{(++)})/T} - 1) \right. \\ &\left. - \sum_{\nu\kappa} \frac{\Sigma_{121'2'}^{\kappa\nu;\nu'\nu''(-)} }{i\omega_n + \omega_{\nu\nu'} + \omega_{\kappa\nu''}^{(--)}} (e^{-(\omega_{\nu\nu'} + \omega_{\kappa\nu''}^{(--)})/T} - 1) \right], \end{aligned}$$

E.L., P.Schuck, Phys. Rev. C 104, 044330 (2021)

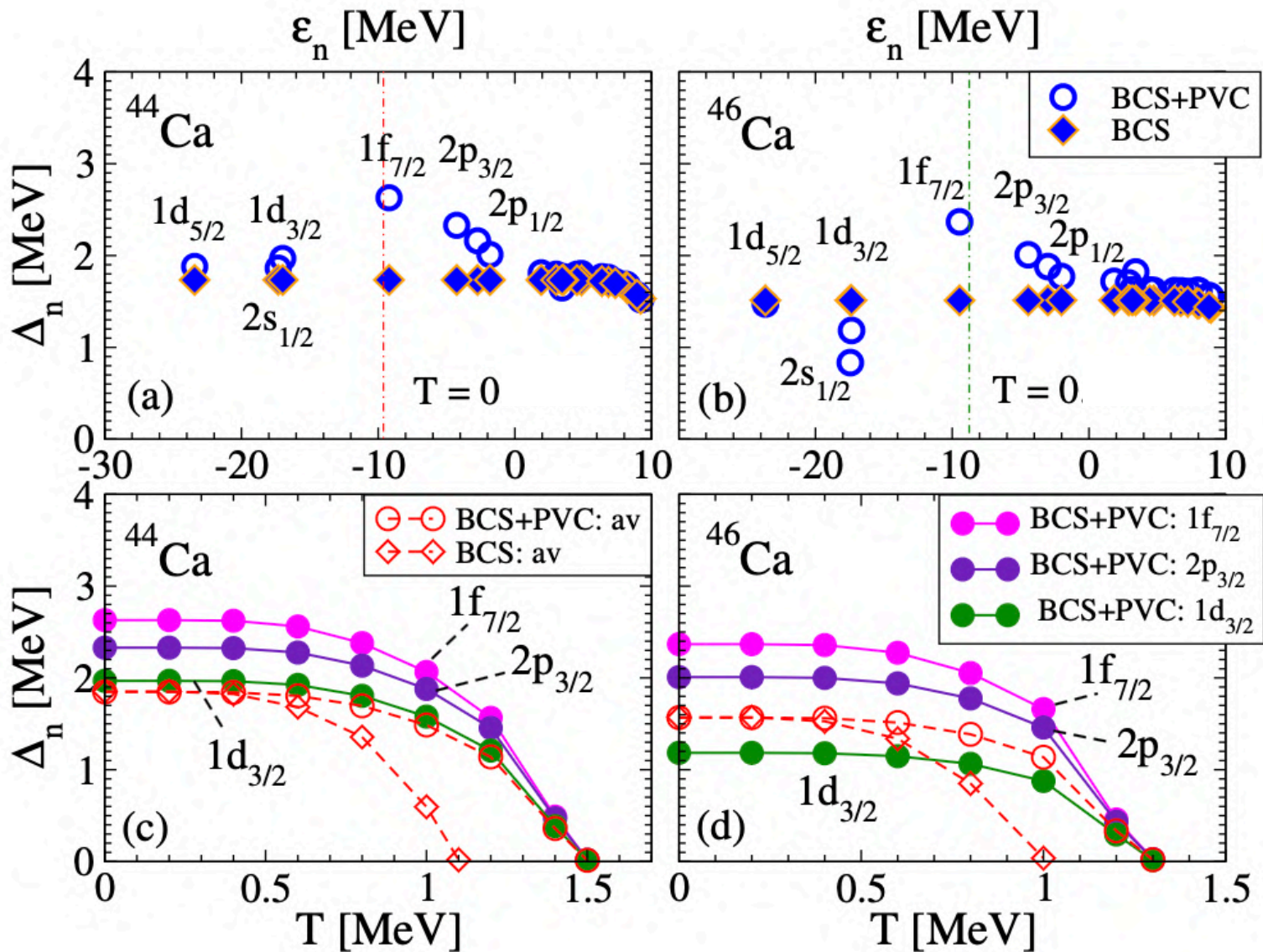
BCS-like gap Eq., but with non-trivial T -dependence in $K^{(r)}$:

$$\Delta_1(T) = - \sum_2 \nu_{1\bar{1}2\bar{2}} \frac{\Delta_2(T)(1 - 2f_2(T))}{2E_2}$$

$$f_1(T) = \frac{1}{\exp(E_1/T) + 1}$$

$$\mathcal{V}_{121'2'} = \frac{1}{2} \left(K_{121'2'}^{(0)} + K_{121'2'}^{(r)}(2\lambda) \right)$$

Pairing gap at $T = 0$, $T > 0$ and critical temperature





Outlook

Summary:

- The relativistic nuclear field theory (RNFT) is formulated and advanced in the Equation of Motion (EOM) framework, with the emphasis on *emergent collectivity*.
- The *emergent collective effects* renormalize interactions in correlated media, underly the spectral fragmentation mechanisms, affect superfluidity and weak decay rates.
- Relativistic NFT is *generalized to finite temperature* and applied to nuclear superfluidity.
- Weak rates at astrophysical conditions are extracted: *the correlations beyond mean field are found significant*.

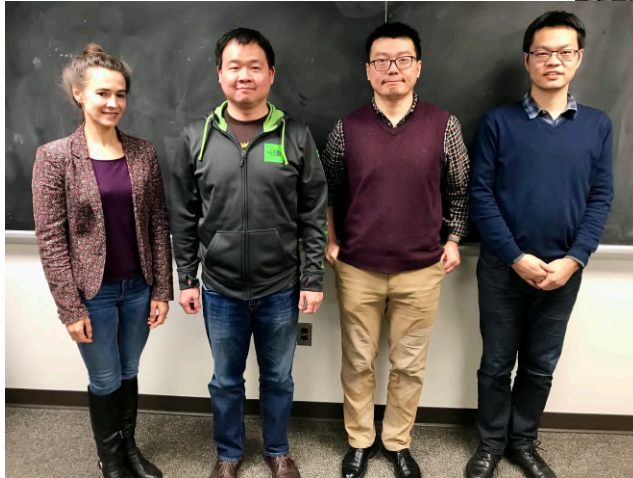
Current and future developments:

- *Deformed nuclei*: correlations vs shapes; first results just released (Yinu Zhang et al.);
- Efficient algorithms; *quantum computing* (Manqoba Hlatshwayo et al.);
- Implementation of the EC rates into the *core-collapse supernovae simulations*;
- Toward an “*ab initio*” description: implementations with bare NN-interactions;
- *Superfluid pairing at $T>0$* to extend the application range (r-process);
- *Relativistic EOM’s, bosonic EOM’s, beyond Standard Model, ...*

Many thanks for collaboration and support:

Yinu Zhang (WMU)
Manqoba Hlatshwayo (WMU)
Herlik Wibowo (AS Taipei)
Caroline Robin (U. Bielefeld & GSI)
Peter Schuck (IPN Orsay)
Peter Ring (TU München)
Tamara Niksic (U Zagreb)

2018:



2017:



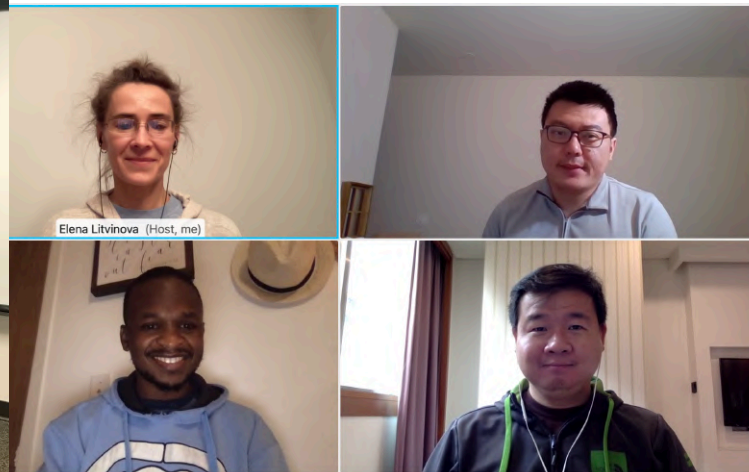
**US-NSF CAREER
PHY-1654379 (2017-2023)**

**US-NSF PHY-2209376
(2022-2025)**

2019-2020:



2020-2022:





Thank you!

